Stochastic Environmental Research and Risk Assessment 14 (2000) 339–369 © Springer-Verlag 2000

Modes of low-frequency climate variability and their relationships with land precipitation and surface temperature: application to the Northern Hemisphere winter climate

L. Terray, C. Cassou

Abstract. Variations in the Earth's climate have had considerable impact on society sectors such as energy, agriculture, fisheries, water resources, and environmental quality. This natural climate variability must be documented and understood in order to assess its potential impacts, its predictability and relationships with human-induced changes. Understanding the mechanisms responsible for natural variability proceeds through a strategy based on the use of a hierarchy of climate models and careful data analysis. In this paper, we examine primarily climate fluctuations on interannual-to-decadal time scales and their climate signature in terms of precipitation and temperature. First, space and time characteristics of two of the major variability modes, the Southern Oscillation (and its associated teleconnection patterns) and the North Atlantic Oscillation, are documented with a focus onto the midlatitudes of the Northern Hemisphere. Then, the current hypothesis regarding the nature of these modes (forced, coupled or internal) are reviewed based on both simulation results and statistical data analyses. Next, we address the potential predictability of seasonal surface temperature and land precipitation using an ensemble of atmospheric model simulations forced by observed sea surface temperatures. Finally, we review the relationships between the atmospheric variability modes and the recent low-frequency trends and suggest a possible influence of anthropogenic effects on these low-frequency variations.

1
Introduction

Humankind lives at the bottom of the sea of air called atmosphere and climate fluctuations are perceived by us mainly as a change in the conditions of this sea's lower layers. It is important to note that these fluctuations (or modes of variability) occur at all time scales and can have very different characteristics: periodic variations, sudden shifts, gradual trends and changes in variability. As a consequence, one has to be cautious in using the mean climate paradigm. The relatively short instrumental record of climate (the last century or so), which includes anthropogenic changes as well as natural variability, does not represent a stationary or steady record. The natural fluctuations introduce a level of unpredictability which limits our ability to forecast future climate change. Quantifying the level of natural variability is thus a necessary prerequisite to the detection of changes due to human activities.

L. Terray, C. Cassou
Climate Modelling and Global Change Project, Cerfacs,
42, Avenue Gaspard Coriolis, F-31057 Toulouse Cedex, France

During the past few decades there has been considerable effort devoted to obtaining a better understanding of natural climate variability on interannual to near decadal (1–10 years) timescales. In his seminal study of global atmospheric modes of low-frequency variability, Walker (1924) identified three large-scale oscillations: the Southern Oscillation (SO), the North Pacific Oscillation (NPO) and the North Atlantic Oscillation (NAO). Following the work of Bjerknes (1969), the link between the SO and the alternation of warm (El Niño) and cold (La Niña) sea surface temperature (SST) anomalies over the eastern equatorial Pacific has been firmly established. They are the corresponding pieces of a coupled ocean-atmosphere climate puzzle termed ENSO (El Niño-Southern Oscillation). In a more recent analysis of Northern Hemisphere teleconnections patterns, Wallace and Gutzler (1981) confirmed the presence of the NAO in both surface and 500-mb data and identified the Pacific North American (PNA) and West Pacific (WP) teleconnection patterns as the two other predominant modes over the North Pacific-American region. In particular, the PNA pattern has been shown to recur frequently in ENSO years (Horel and Wallace, 1981). Two of these modes are the primary focus of this paper: the SO and its associated extratropical teleconnection patterns and the NAO. The first one has a strong tropical connection associated with changes in tropical convection. The second one is associated with changes in strength and location of the dominant zonal flows in middle and high latitudes of the North Atlantic region. As we are mainly interested in the midlatitude climate in this paper, we will concentrate on the remote influence of the (EN)SO on Northern Hemisphere variability modes as well as on the NAO. In this paper, we assume that the relationship between the opposite phases of the SO and El Niño and La Niña events is sufficiently strong. Consequently, we will refer equivalently to the low phase of the SO or warm ENSO events and to the high phase of the SO or cold ENSO events. The focus on periods less than 10 years relies on the fact that these explain more than 75% of the total variance. Moreover, potential predictability in this forecast range offers the most direct benefit to decision makers.

While ENSO is a large-scale coupled ocean-atmosphere tropical phenomenon, the NAO results from the complex aggregation of mid-latitude weather variations, which may also be influenced by oceanic or stratospheric conditions. The atmospheric part of the former consists of a global scale, predominantly standing wave with centers of action in surface pressure over Indonesia and the Central-Eastern tropical Pacific. Tropical SST changes influence the atmosphere through surface fluxes of heat, moisture and momentum leading to an adjustment of the tropical atmospheric circulation in a thermally direct sense. Changes in convective activity, heating, low-level convergence and upper-level divergence alter the generation of the horizontal component of atmospheric vorticity, leading to the forcing of large-scale atmospheric Rossby waves propagating out of the Tropics. These waves interact with the planetary stationary waves and transient phenomena at higher latitudes. They are the main cause behind teleconnection patterns which represent the relationships in the variability of large-scale features of the atmospheric circulation as well as tropical and extra-tropical precipitation and surface temperature relationships.

The latter is characterized by a large scale alternation of atmospheric mass with centers of action near the Icelandic Low and the Azores High. It is robustly present in every month of the year (although it is more pronounced during winter) (Barnston and Livezey, 1997) and accounts for the largest fraction of interannual variability in monthly North Atlantic sea level pressure (SLP) (Rogers, 1990). It is associated with concomitant fluctuations in rainfall and winter

surface air temperature (SAT) reaching eastward to central Europe, southward to subtropical West Africa and westward to North America. For instance, high index winters (pressure is anomalously low near Iceland while it is anomalously high near the Azores) have stronger outflow of cold Arctic air over Greenland and stronger advection of warm maritime air over Europe, resulting in winter air temperatures being out of phase on either side of Iceland (the so-called temperature seasaw between Greenland and Scandinavia) (Van Loon and Rogers, 1978; and references therein).

However, the mechanisms governing these climatic fluctuations are still not fully understood. A number of recent studies have sought to identify the nature of the variability at different timescales by analyzing both observational records and results of climate model simulations. The purpose of this paper is: (1) to explore various ways of describing two major modes of low-frequency climate variability, the SO and the NAO, (2) to describe their signatures in terms of surface temperature and precipitation with a strong focus onto the midlatitudes of the Northern Hemisphere, (3) to assess how much of the regional climate variability is due to ocean surface forcing using ensemble of atmospheric model simulations, (4) to discuss possible links between climate change and these two modes of variability.

Section 2 describes the datasets used in this study as well as the modelling and statistical tools.

Section 3 describes the spatial and temporal structure of the Southern Oscillation (SO) and NAO modes using mostly atmospheric data and the NCEP reanalysis. Observed teleconnections are documented mainly in terms of surface temperature and precipitation as well as relationships between the tropics and extratropics. The nature of these modes is discussed in Sect. 4 based on atmospheric general circulation model (AGCM) experiments following by an assessment of the associated potential predictability. Section 5 presents a short review, based on recent studies of various authors, of the potential interaction between the low-frequency variability modes and the recent warming trends over the Northern Hemisphere, often associated with the anthropogenic climate change. Finally, Sect. 6 summarizes the major findings of this study.

2
Data, statistical methods and model used in this study

2.1
Datasets

In this study, we have used the Jones et al. (1986) temperature and pressure data set which is freely available from the web at http://www.cru.uea.ac.uk/. The pressure data set contains northern hemisphere monthly mean-sea-level pressure (MSLP) data on a 5° latitude by 10° longitude grid-point basis. The sources of the original chart data are given in Jones (1987). The temperature data set is a combination of land SAT (observed at 2 m above the ground) anomalies (Jones, 1994) and SST anomalies (Parker et al., 1995) on a 5° by 5° grid-box basis. In this work, we have only considered data after 1900 in order to get more reliable results. We have also used an historic monthly precipitation dataset for global land areas from 1900 to 1998 gridded at 5° resolution ('g55wld0098.dat' (Version 1.0) constructed and supplied by Dr Mike Hulme at the Climatic Research Unit, University of East Anglia, Norwich, UK. This work has been supported by the UK Department of the Environment, Transport and the Regions (Contract EPG 1/1/48). (Hulme, 1992). We have also used classical indexes for both the SO and the

NAO: the Southern Oscillation Index (SOI) which is the normalized difference between normalized MSLP monthly time series, Tahiti minus Darwin, (Ropelewski and Jones, 1987) and the winter (DJFM) NAO Index (NAOI) as defined by Hurrel (1995), the difference of standardized SLP between the Azores and Iceland (Jones et al., 1997). Both indexes have been obtained from the CRU website given above. Finally, we have also used the NCEP reanalysis over the 1958–1997 period (1959–1998 for winter). These have been downloaded from the LDEO website http://ingrid.ldgo.columbia.edu/SOURCES/ (Kalnay et al., 1996).

2.2 Statistical methods

A common method to study the variability of climate variables is the empirical orthogonal function (EOF) analysis which has been widely used in geophysics science (Bretherton et al., 1992; Deser and Blackmon, 1993). EOF analysis applies to a space- and time-dependent field with zero temporal mean. The variance-covariance matrix of the field is diagonalized, yielding a set of eigenvalues and corresponding eigenvectors. Each eigenvector (or EOF) can be viewed as a spatial pattern which evolves in time according to an expansion coefficient (or principal component, PC). The latter can be obtained by projecting the eigenvector onto the original field. The fraction of the total variance explained by a given EOF is proportional to its associated eigenvalue. The modes of variability (the eigenvalues and associated EOF and PC) are ranked by explained fraction of total variance in decreasing order.

All the spectral analyses performed in this study are based on the Thompson's multitaper method (Thompson, 1982; Dettinger et al., 1995; Vautard et al., 1989). The confidence levels are obtained relative to an estimated red noise background (Mann and Lees, 1996).

2.3 The ARPEGE model

The atmospheric GCM used in the present study is derived from the ARPEGE/IFS forecast model and is described by Déqué et al. (1994). It is a spectral model and uses a two time level semi lagrangian scheme with semi-implicit time discretization of the primitive equations. The present version is used at spectral T63 triangular horizontal truncation. Diabatic fluxes and non linear terms are calculated on a gaussian grid of about 2.8° latitude by 2.8° longitude The vertical is discretized over 31 levels (20 levels in the troposphere) using a progressive vertical hybrid coordinate extending from the ground up to about 34 km (7.35 hPa). The model time step for this resolution and time discretization scheme is 30 min. The model has a comprehensive package of physical parameterizations including a detailed treatment of the land surface processes via the ISBA model (Noilhan and Planton, 1989). The convection is represented by a mass flux scheme with detrainment as proposed by Bougeault (1995). The radiative package follows the Fouquart and Morcrette's scheme (Morcrette, 1990). Parameterizations of boundary layer and turbulence are based on vertical exchange coefficients computed as functions of the local Richardson number according to the Louis et al.'s (1982) method.

3 Spatio-temporal properties of low-frequency climate variability modes

There is considerable debate on the best way to characterize low-frequency variability modes. Indeed, this is related to the poor knowledge of the nature and main physical mechanisms of these modes. For instance, current research ques-

tions are the following: are these modes really independent, are they truly coupled modes of the climate system or rather a selective response to the atmospheric noise stochastic forcing, what influence does global warming have on their amplitude and scale, etc. The large scale patterns of atmospheric circulation determine the distributions of surface temperature and precipitation over land. In this section, different methods are used to investigate how much regional variability in surface temperature and rainfall can be accounted for by the low-frequency variability modes. The first approach consists in establishing time series for each of the modes and assess their impacts using linear regression on time series of global atmospheric rainfall and surface temperature. Several options regarding the choice of the most appropriate time series are discussed and compared. The second approach is based on the use of mathematical tools such as empirical orthogonal function (EOF) analysis. Both methods have severe limitations as the relationships between the low-frequency modes and the climate variables of interest are non-linear. More suitable in this context are the family of techniques designed to quantify the probability distribution of the state of the atmosphere in multidimensional phase space. Here the Ward automatic clustering scheme has been considered as an alternative to linear regression or EOF-based methods to extract the main variability patterns (Cheng and Wallace, 1993; Martineu et al., 1999). Its advantage is that no symmetry or orthogonality constraints are required on variability patterns. However, these types of methods need large sample sizes to produce stable and reproducible results.

3.1
Sea-level-pressure indexes of the SO and NAO

Simple climatic indexes have traditionally been used to characterize the signature of atmospheric variability modes. For instance, the SOI has been used to quantify the intensity of the equatorial easterlies in the tropical Pacific, which can be viewed as the lower branch of an east-west zonal "Walker Circulation" driven by the basin-scale SST gradient (Walker, 1924; Bjerknes, 1969). The coupling between the circulation field of Walker's SO and the zonal SST gradient in the equatorial Pacific provides the main feedback mechanism at the root of the ENSO phenomenon. Another example is the NAOI which summarizes the mean westerly flow over the North Atlantic region (Walker and Bliss, 1932; Bjerknes, 1964). Figure 1 shows both the SOI and NAOI as well as low-frequency trends depicted by 6-year running means. Both time series exhibit intervals of extended residence both above and below the mean (clearly visible in the low-frequency curves). Of particular interest are the last 20 years for the SOI (negative trend, strong ENSO events) and the 1972–1995 period (above the mean) and 1950–1970 period (below the mean) for the NAOI. The interpretation of these features in terms of deterministic causes and the question of stationarity of these time series are the subject of intense debate among climate statisticians (e.g Wunsch, 1999 and references therein). The energy spectra of the SOI and NAOI are shown in Fig. 2. The NAOI spectrum is nearly white with energy concentration in the quasi-biennal (2.4 years) and near-decadal (8 years) bands (Hurrel and Van Loon, 1997) while the SOI one is slightly redder with a strong harmonic peak around 3.7 years. Energy in both time series occurs at the highest frequencies (in the interannual to near-decadal bands). Longer records for tracking the NAO have been constructed from tree-ring based data (1701–1980) (Cook et al., 1998) and Greenland ice cores (Appenzeller et al., 1998). Wavelet analyses of the proxy data-based indexes shows essentially a white spectrum but for the last century where concentration of spectral power at a 70-year period occurs leading to slight reddening. In the SO

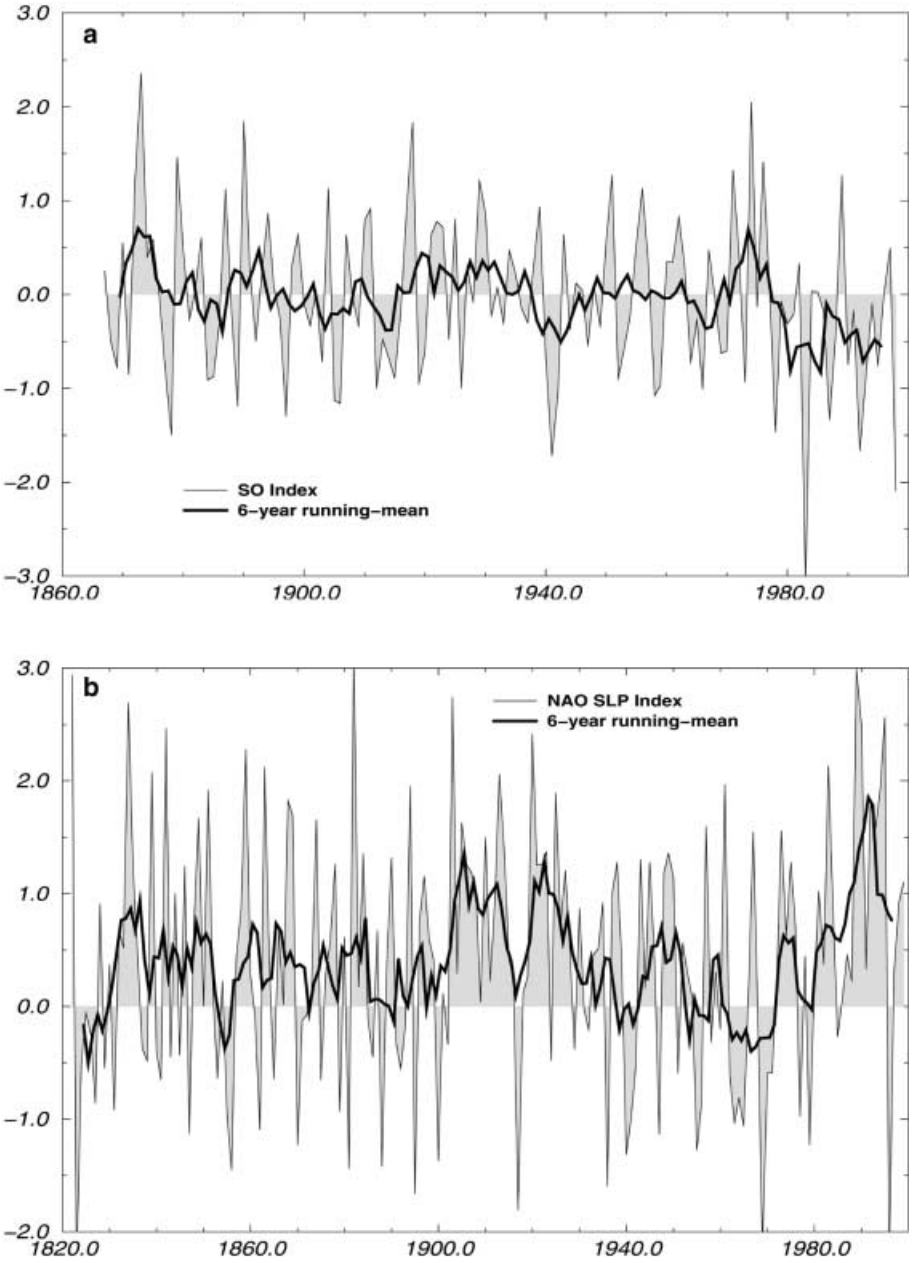

Fig. 1a, b. Time series of the (**a**) Southern Oscillation index (SOI) between 1866 and 1998 and (**b**) North Atlantic Oscillation index (NAOI) between 1821 and 1997. The SOI and the NAOI are defined here as the winter average of monthly values (NDJF and DJFM, respectively). Low-frequency trends are indicated by the 6-year running median (thick line)

case, coral data offers the opportunity for long paleographic reconstructions of SST from several sites in the different regions of the tropical Pacific. For instance, a 370-year record of $\delta^{18}O$ (with annual resolution) from the eastern Pacific indicates significant decadal scale variability in SST (Dunbar et al., 1994). Analysis

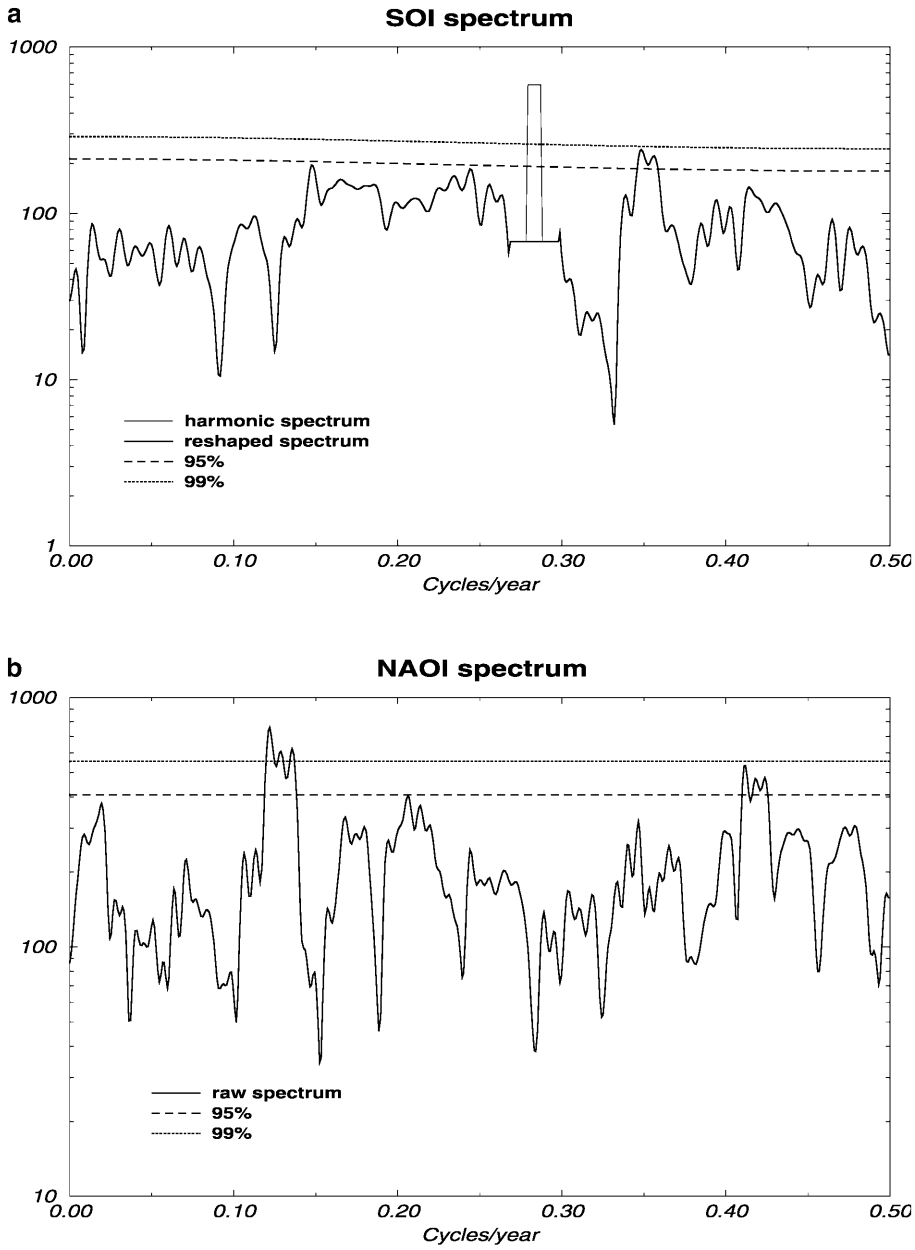

Fig. 2a, b. Multi-taper spectral density estimate as a function of angular frequency of the (**a**) SOI and (**b**) NAOI indexes. 95% and 99% confidence intervals are estimated relatively to pure red noise (AR(1) process)

of variability of both the NAO and SO phenomena over the past several centuries will require extensive use of new paleoclimatic data in order to yield insight into the past behavior of specific components of the global climate system.

Regression coefficients are now calculated using linear regression between the SOI and NAOI and the winter global land rainfall and air and surface temperature fields. The SOI is here defined as the winter (NDJF) average of the monthly index.

The various regression coefficients are shown in Figs. 3 and 4 and indicate the regions which are influenced by the modes and to which degree. While the SO affects much of the global tropics and large portions of the extratropics throughout the year, the NAO is strongly focused over the North Atlantic ans surrounding continental regions and is primarily a winter and spring phenomenon.

Regional surface temperature relationships with the SO are presented in Fig. 3a. The buildup of positive tropical SST anomalies which accompanies the low phase of the SO results in above-normal land SAT for many areas in the

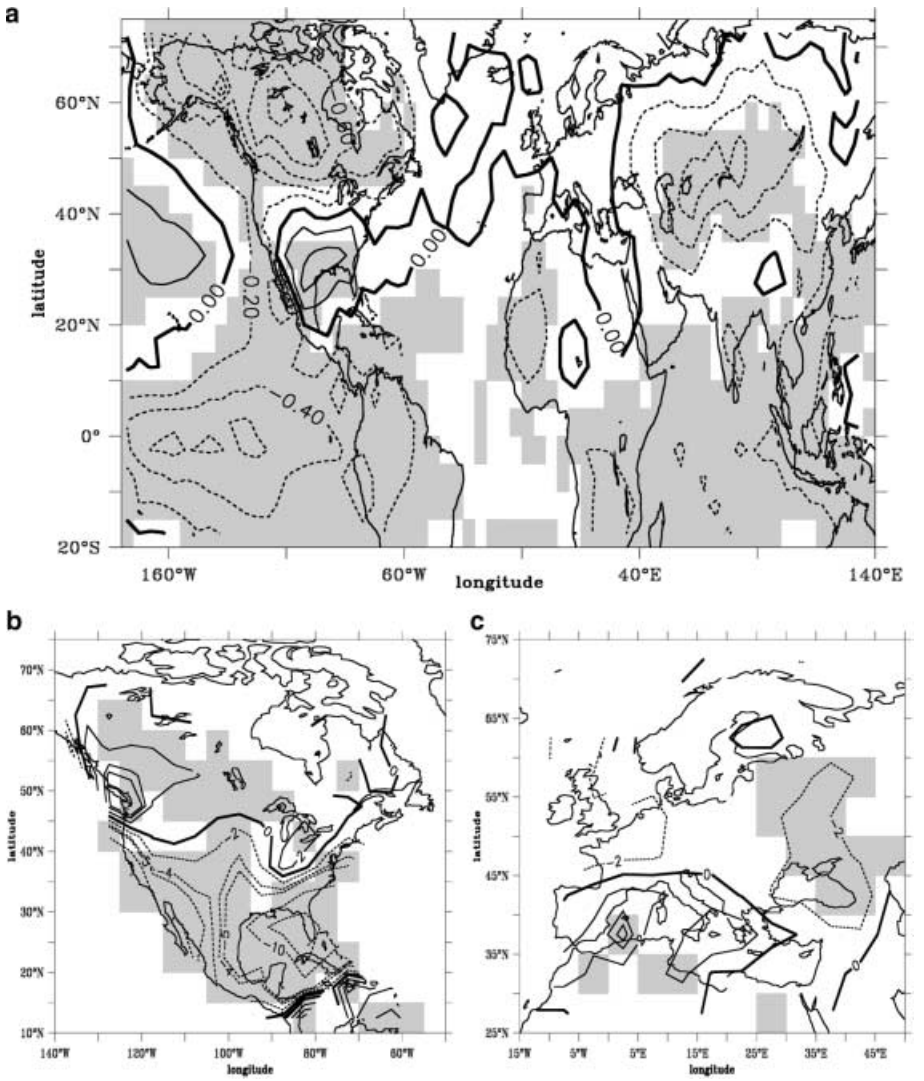

Fig. 3a–c. Regression of the time series of the observed winter (NDJF) SOI index as defined in Fig. 1, onto (**a**) observed winter land air and sea surface temperature anomalies and (**b, c**) observed winter land precipitation for the American and European sectors. Regression periods are 1900–1993 for temperature and 1900–1998 for precipitation. Shading indicates areas exceeding the 95% confidence level of non-zero correlation using a 2-tailed t-test. Units are in K and mm and correspond to an SOI anomaly of one standard deviation

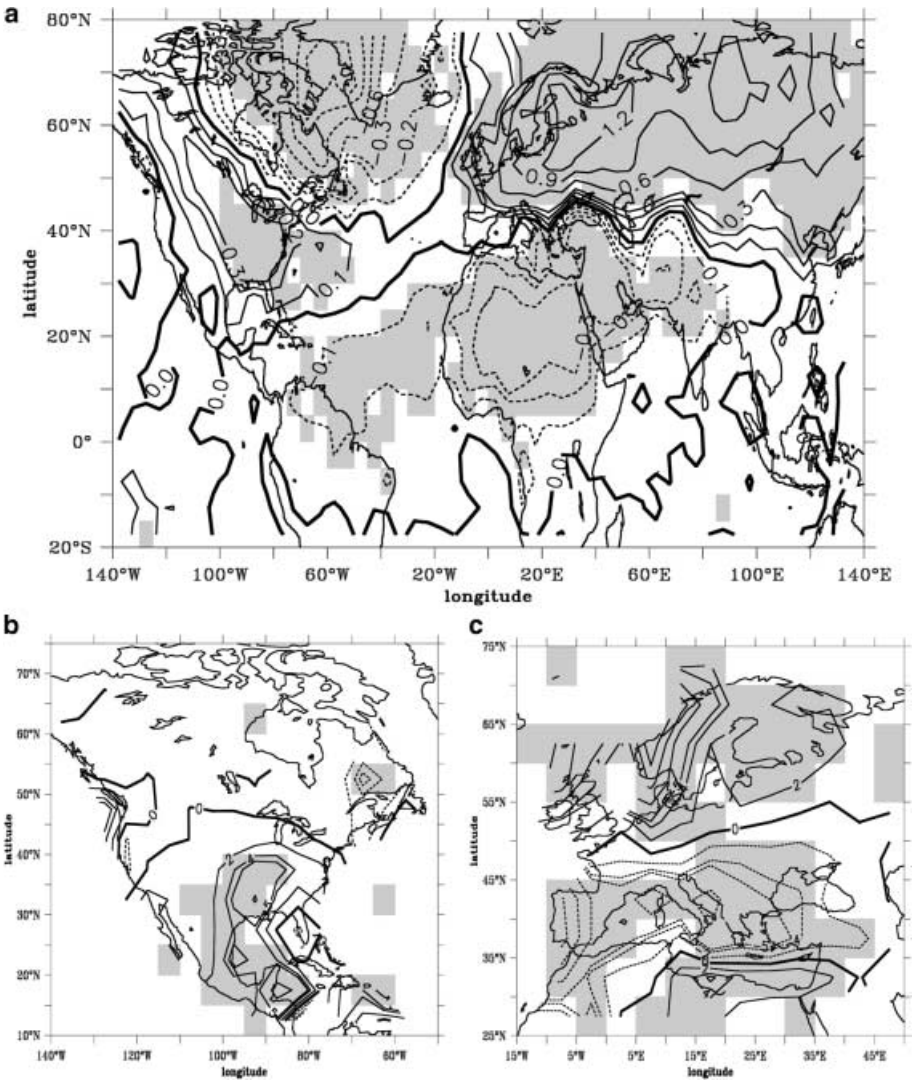

Fig. 4a–c. Regression of the time series of the observed winter (DJFM) NAOI index as defined in Fig. 1, onto (**a**) observed winter land air and sea surface temperature anomalies and (**b, c**) observed winter land precipitation for the American and European sectors. Regression periods are 1900–1993 for temperature and 1900–1998 for precipitation. Shading indicates areas exceeding the 95% confidence level of non-zero correlation using a 2-tailed t-test. Units are in K and mm and correspond to an NAOI anomaly of one standard deviation

global tropics including western and central South America, the Central America-Caribbean islands, western and southeastern Africa, southeast Asia and northern Australia. Extensive work on the detailed timing and seasonal stratification of the SO-temperature relationships has been performed by Van Loon and Madden (1981), Kiladis and Diaz (1989) and Halpert and Ropelewski (1992) among many others. While most of the SO-temperature relationships in the Tropics can be related to either shifts in convection patterns or to the direct impact of SST fluctuations, changes in large-scale flow patterns due to the tropical forcing are responsible for SO-temperature relationships in the extratropics. Northwestern

North America and the southeastern United States (US) have strong SO-temperature relationships while that of eastern Canada has a weaker amplitude. Forcing of the PNA pattern (i.e with a trough in the Gulf of Alaska, a ridge over northwestern North America and a trough in the southeastern US) has often been associated with the low phase of the SO. Its related SAT anomalies are consistent with the regression pattern (in case of the low phase of the SO, above normal temperatures in Alaska, western and eastern Canada with below normal temperatures in the southeastern US). While the results shown here indicate that the SO-temperature linear relationships are very shallow, if at all existing, over Europe, a large-scale and statistically significant region does appear over Central Asia. This anomaly across Eurasia at latitudes near 50°N appeared in particular for the 1982–1983 warm ENSO episode (Quiroz, 1983). The surprising global result needs further confirmation with a different dataset and might indicate a decadal variation in SO-related teleconnections.

The regression pattern for precipitation indicates a clear out-of-phase relationships between Alaska, the Pacific Northwest and southern Canada on one hand, and the southern part of the US (with maxima in the Gulf of Mexico and California regions) on the other hand (Fig. 3b). Note, however, that the SO-precipitation relationships at high latitude (>45°N) is much less consistent than its lower latitude counterpart. This might indicate the strong sensitivity of regional precipitation to the exact location and strength of the SO-related PNA pattern. The strong response in the Gulf of Mexico region might be due to a direct link to SO forcing rather than a teleconnection through the PNA pattern. Enhanced convection in the equatorial Pacific is related to a stronger subtropical jet, and hence, a tendency for increased storm-track activity and precipitation in the Gulf (low phase of the SO). Furthermore, the presence of warm SST anomalies off the southern California coast may be partly responsible for the precipitation increase over the southwestern US. As for Europe, Fig. 3c suggests that precipitation changes might be associated with the SO over central Russia, north of the Black Sea (increased rainfall for the low phase of the SO). The linear response over western Europe is weak and not significant.

As the NAO reflects variations in the strength and orientation of mid-Atlantic westerlies which dictate heat and moisture flux trajectories, fluctuations of the NAOI are expected to directly impact the regional patterns of surface temperature and precipitation. Continental temperature changes of large amplitude (>1 °C) associated with a one standard deviation in the NAOI occur over Greenland and northern Canada and extend from northern Europe across much of Eurasia. They illustrate the temperature seasaw with negative anomalies over Greenland and positive ones over Scandinavia in case of a positive NAOI. Weaker amplitude changes (but still statistically significant) over the eastern US (in phase with northern Europe) and from northern and central Africa to the Middle East (in phase with Greenland) are also clearly depicted in Fig. 4a. The regression pattern over the ocean shows the so-called north Atlantic tripole with negative centers in the subtropics and south of Greenland and positive centers off the east coast of the US and in the Norwegian sea (positive NAOI case) (Bjerknes, 1964; Sutton and Allen, 1997). There is also a cold signal over the eastern Mediterranean Sea which can affect the saturation water vapor of the overlying atmosphere and thereby, impact the low-pressure systems which migrate towards the Middle East.

Changes in precipitation are observed over the southeast US and in a small area in eastern Canada (Fig. 4b). Over the european continent, a clear out-of-phase relationship between a northern region from the British Isles through Scandinavia and much of central and southern Europe emerges in agreement with

changes in the mean circulation patterns and related shifts in storm-tracks characteristics (Fig. 4b). In particular, a study by Cullen and deMenocal (1999) has shown that 50% of the Turkish winter precipitation variability can be attributed to the NAO. While mid and high latitudes are characterized by this meridional dipole, the subtropics present a more zonal out-of-phase relationship between northwest (Morocco) and northeast (Egypt) Africa. For instance, Lamb and Peppler (1991) have documented a strong association between the NAO and wintertime precipitation in Morocco.

3.2
Cluster analysis of the mean sea level pressure field

The Ward automatic clustering scheme has been applied to the total ensemble of observed atmospheric states over the 1900–1995 winter season. Each individual state is the observed realization of one particular event (December, January or February month for a given winter) for the MSLP field. The coordinates of the state vector are its N monthly mean anomaly values on the N grid points of the appropriate geographical zone. In this study, two different regions have been selected: the North Atlantic/European (NAE) [70°W–40°E; 15°N–85°N] and the North Pacific-American (NPA) [140°E–60°W; 15°N–85°N] sectors. Each resulting cluster is defined by its ensemble mean (or centroid) and spread as well as the number of realizations of each winter aggregated in the cluster. The statistical significance of a given cluster is evaluated using Student (resp.: Fischer) tests to compare the ensemble mean (resp.: variance) of the cluster to the ensemble mean (resp.: variance) of the initial population (at the 95% confidence level). This statistical procedure is applied either to the classified variable (the MSLP) to check the robustness of the clusters or to another variable (surface temperature or rainfall) to measure its relationship with the MSLP patterns resulting from the clustering scheme.

Figure 5 shows the spatial patterns for the centroids associated with each of the four representative clusters coming from the analysis of winter MSLP data for the NAE region. The first cluster defines a high-pressure center over the central North Atlantic while the second one depicts an out-of-phase relationship between the Greenland Sea and North-eastern Europe. The last two clusters resemble contrasting polarities of the NAO. They also indicate significant non-linearity in the dominant spatial patterns of variability as the high-pressure center is shifted eastward in the positive NAO phase. The percentages of area covered with significant anomalies of mean and variance exceed the significance thresholds for the last three clusters. The robustness of the two NAO-related clusters has been successfully tested by carrying out the clustering analysis on the NCEP data for the 1958–1997 period (not shown). The same clusters emerged, though with slightly different occupation percentages. In Fig. 6, we document the time history of the occurrence of the four clusters, over our 95-winter dataset. There is strong interannual variability in the occurrence of clusters 1, 3 and 4. In particular, and in agreement with the NAOI time series, negative NAO phases are predominant from the 1940s to the 1970s while the occurrence of positive NAO phases strongly increases after 1970. Maps of associated patterns of surface temperature and precipitation are shown in Figs. 7 and 8 for the two NAO-related clusters, respectively. The geographical SAT patterns are remarkably symmetric over continental areas, especially over Europe, North Africa and the Middle East regions. It also applies to the North American continent with the exception of the western US where both clusters are associated with negative temperature anomalies (weakly significant). The maxima amplitude is usually smaller in the negative

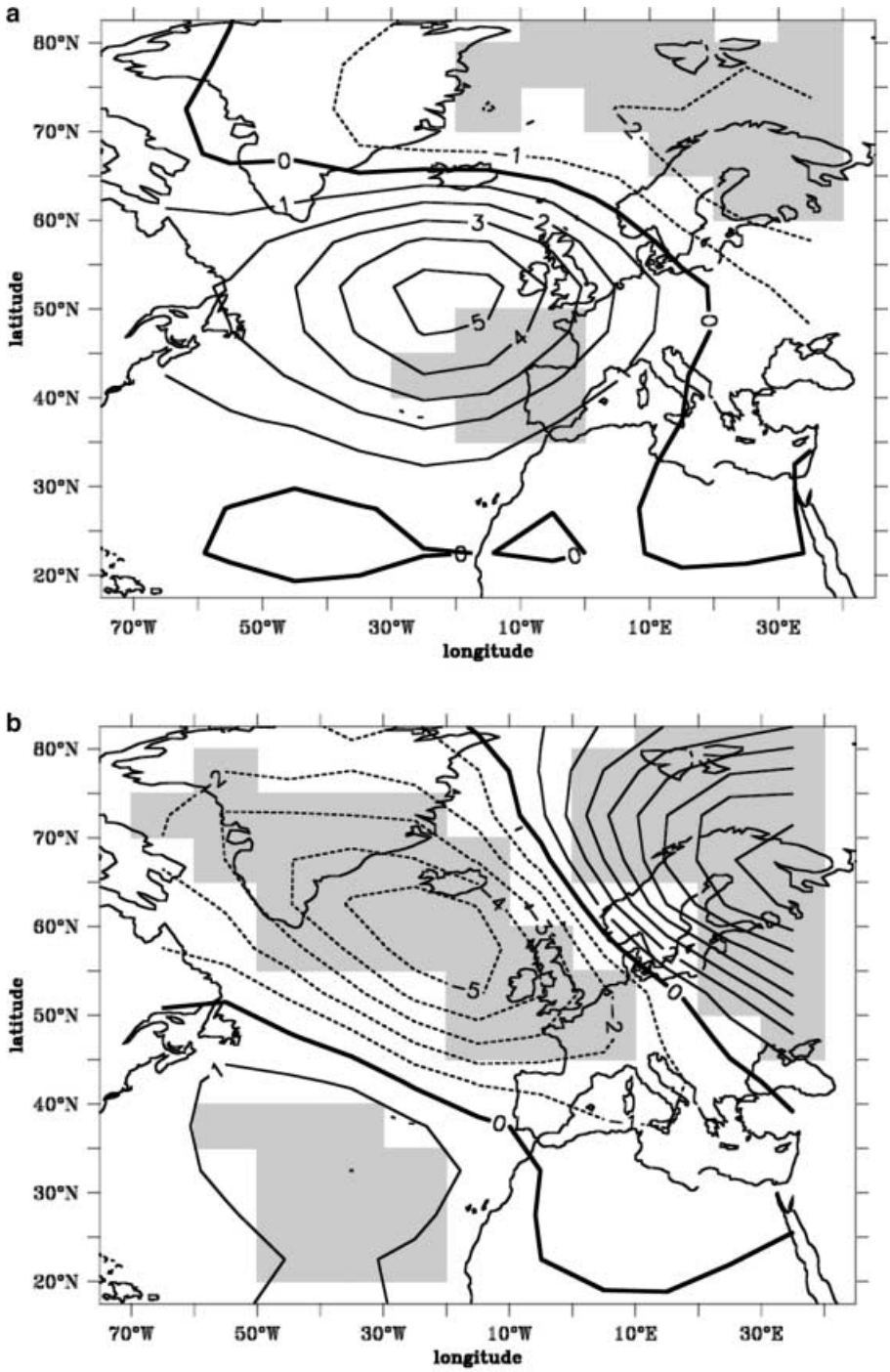

Fig. 5a–d. Centroids of clusters number (**a**) 1, (**b**) 2, (**c**) 3 and (**d**) 4 of the winter (DJF) North Atlantic-European sector mean sea level pressure field clustering analysis. Shading indicates the regions where both the mean and variance of the relevant cluster are significant at the 95% level

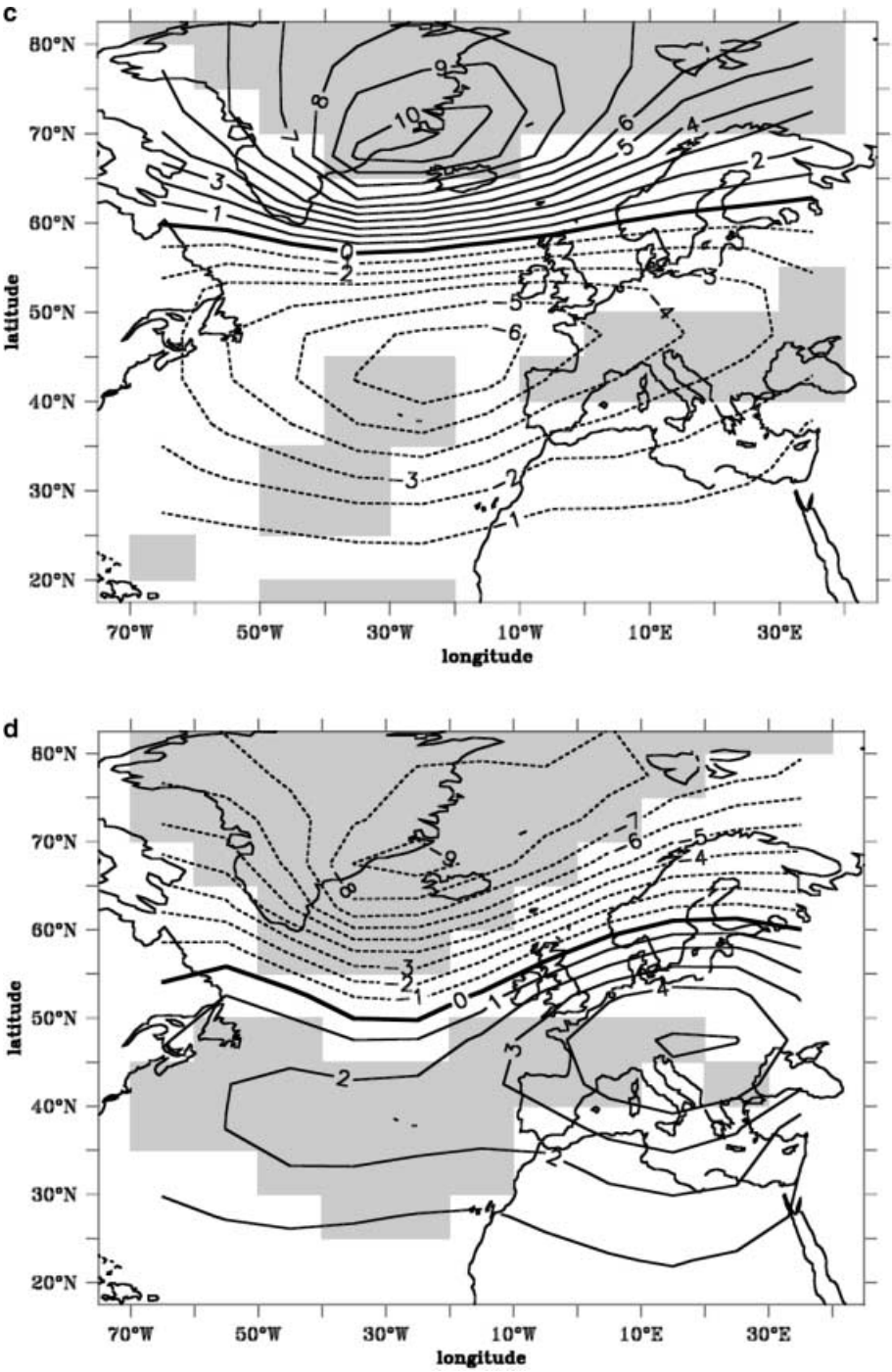

Fig. 5a–d. (Contd).

NAO phase, in particular over Greenland and Scandinavia. Over the North Atlantic ocean, the tripole structure for the negative NAO phase is more confined to the coast with smaller amplitude for the lobe located off the east coast of the US

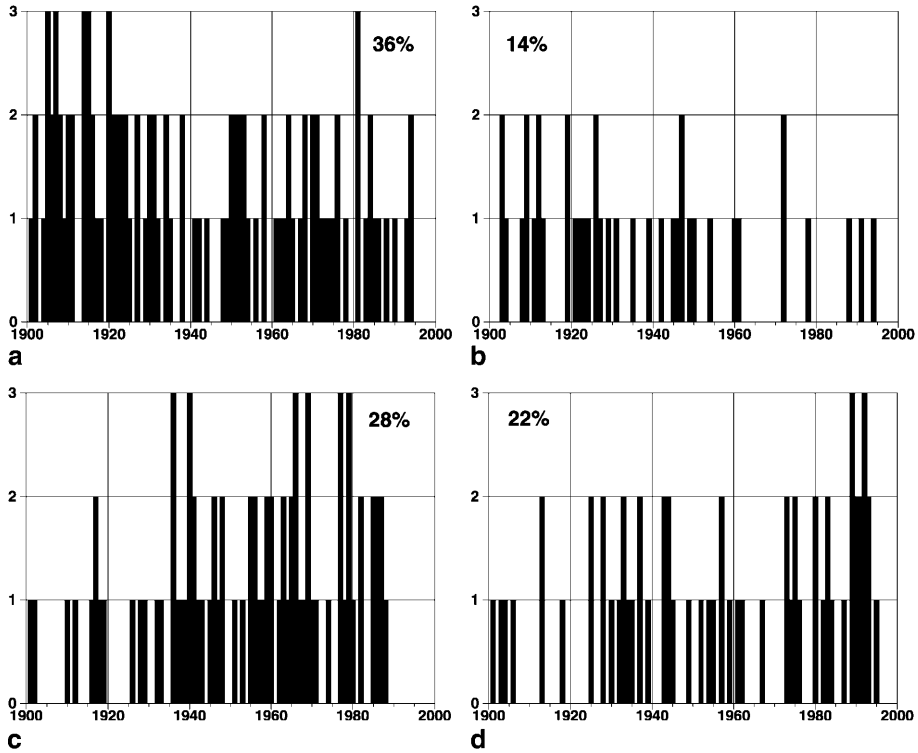

Fig. 6a–d. Time evolution of the 4 clusters (**a, b, c** and **d**, respectively) defined by the clustering analysis performed over the North Atlantic-European sector. For each cluster, the vertical bars indicate the number of months relative to each winter where the cluster is present. The percentage gives the global population of a given cluster over the whole period

(which extends to the eastern Atlantic in the positive NAO cluster with a larger amplitude, up to 0.6 K). The relationships between the modes of atmospheric variability and the surface temperature outlined by the clustering analysis are very close to those depicted by linear regression with the exception of the stronger amplitude of the high latitude maxima associated with the positive NAO phase. The land rainfall patterns associated with the two NAO-related clusters are strongly symmetric over the NAE region and in very good agreement with the linear regression results, in terms of both structure and amplitude. Areas of significance are much smaller over the North American continent and display the out-of-phase relationships already shown in the linear regression results.

The clustering results over the NPA sector mainly outline the PNA response to ENSO warm or cold events. Figure 9 presents the spatial patterns and time evolution of the two clusters associated with the opposite phases of the SO (the two other clusters are not significant). The structure of the warm ENSO phase anomalies (or low phase of the SO) is consistent with a deeper Aleutian low center shifted towards the US west coast. In contrast, the ENSO cold phase pattern indicates weakening of the Aleutian low's central pressure with a slight southward shift. The SO low-phase anomalies display essentially a monopolar structure while the high-phase ones project instead on the PNA teleconnection mode (with centers of action lying along a great circle, North Pacific, northwest Canada and the southeastern US). The negative center has a zonally elongated structure,

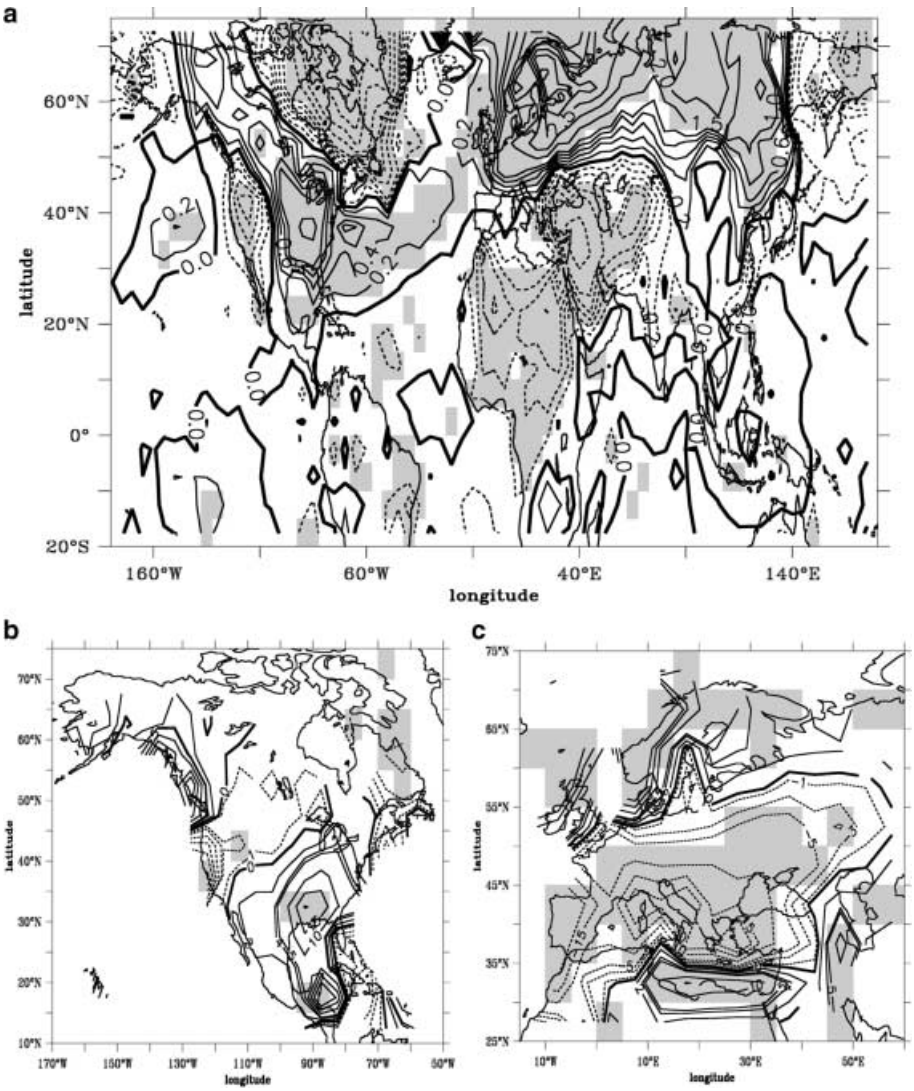

Fig. 7a–c. Patterns of winter (**a**) Northern Hemisphere land surface air and sea surface temperature and (**b, c**) land precipitation for the Pacific North American and North Atlantic-European sectors, respectively, associated with the cluster representing the positive phase of the NAO (Fig. 5d). Shading indicates the regions where both the mean and variance of the climate variable composite are significant at the 95% level. Units are in K and mm

raising the question of the possible hemispheric nature of the mode. The low-phase SO cluster occurred rather frequently at the beginning (1910–1940) and end (1970–1995) of the period while the high-phase one is well represented after 1930, with an increase after 1960 (with the highest presence rate in the 1970s corresponding to the occurrence of several cold ENSO events). The tendencies toward lower ENSO activity through the middle part of the century and more frequent events recently have been firmly established in recent studies (Trenberth and Shea, 1987; Trenberth and Hurrel, 1994).

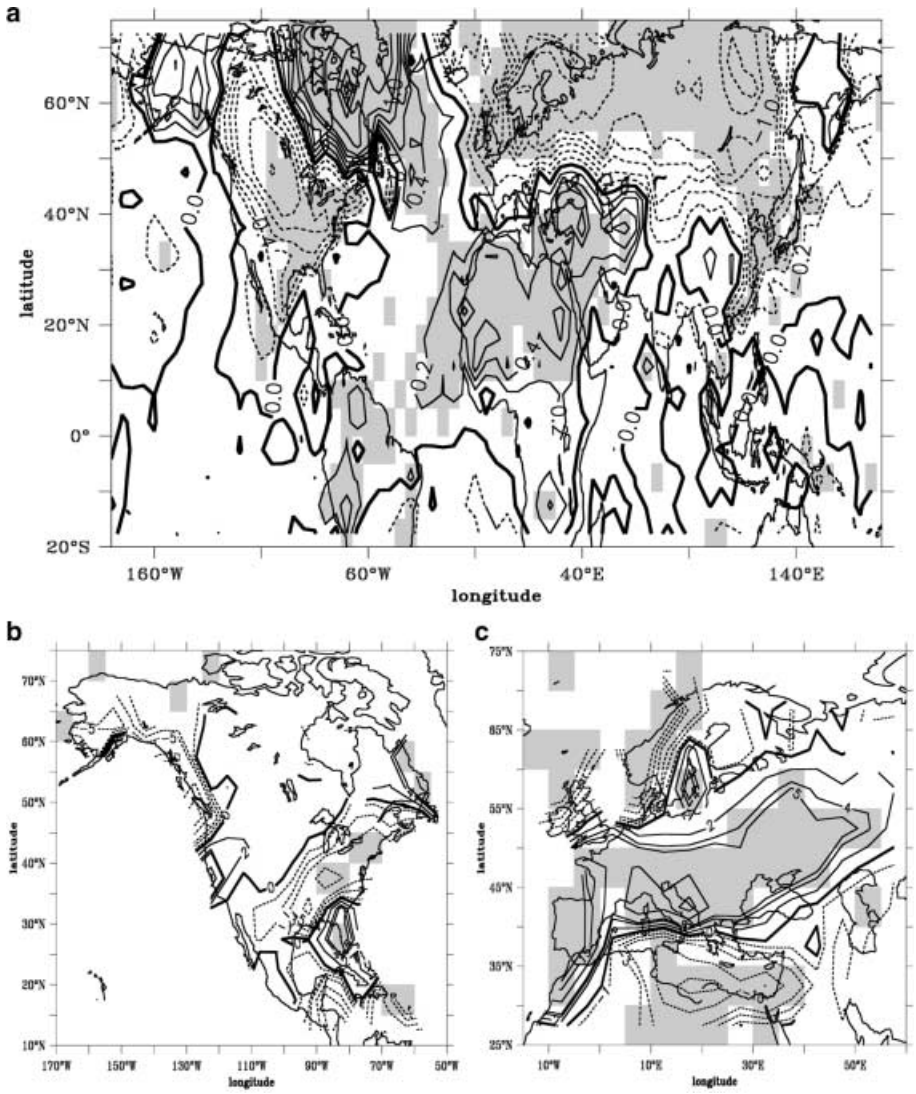

Fig. 8a–c. Patterns of winter (**a**) Northern Hemisphere land surface air and sea surface temperature and (**b, c**) land precipitation for the Pacific North American and North Atlantic-European sectors, respectively, associated with the cluster representing the negative phase of the NAO (Fig. 5c). Shading indicates the regions where both the mean and variance of the climate variable composite are significant at the 95% level. Units are in K and mm

The surface temperature and precipitation response to opposite phases of the SO are presented in Figs. 10 and 11, respectively. The tropical response in surface temperature with respect to the SO phase is not linear due to the relationship between deep convection areas and underlying SSTs. The SO low phase is associated with above normal SSTs in the eastern and central Pacific and warm surface temperature anomalies over most of the tropical band. In contrast, the signal associated with the SO high phase is weak in the tropics outside of the eastern Pacific. There is also clear evidence for non linearity in the North American

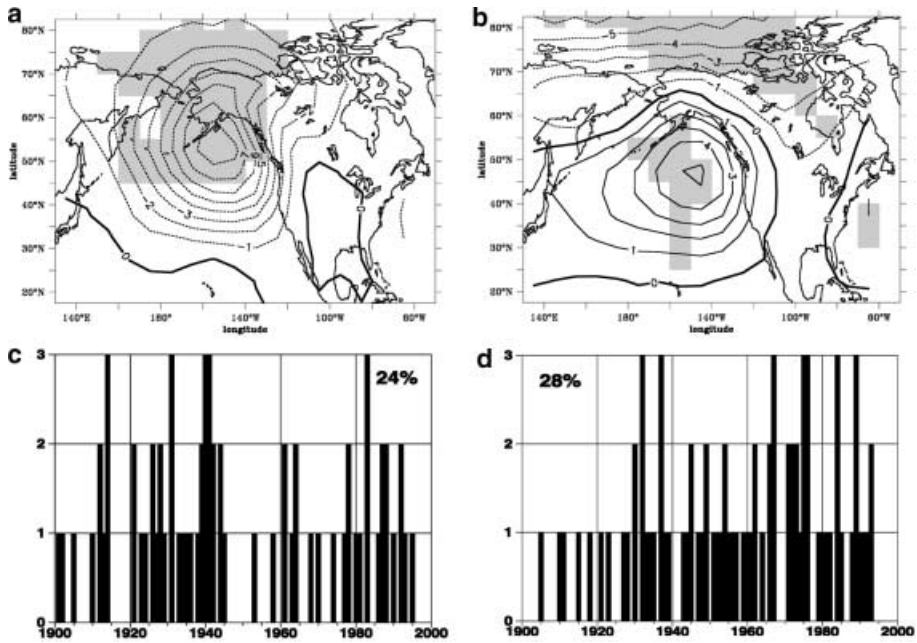

Fig. 9a–d. Centroids (**a**), (**b**) and time evolution (as in Fig. 6) (**c, d**) of clusters number 1 and 2 associated with the low and high phase of the SO, respectively, defined by the mean sea level pressure clustering analysis performed over the Pacific North American sector

climate sensitivity to the SO phase. For instance, the maximum warm SAT anomaly during the SO low phase is located over the northern US, southern and western Canada up to Alaska while the anomalies for these regions are of the same sign (but for Alaska) and not significant in the high phase case. Similarly, the SO high phase SAT maximum is over the Southern Plains and the Midwest and correspond to warm and weakly significant anomalies in the low phase case. Seen in conjunction, the temperature maps indicate that only small areas of the Gulf coast and northwestern US show symmetric relationships between opposite SO phases. The rainfall patterns associated with the SO low phase display a tilted dipole with positive anomalies over the southeastern US and negative ones along an axis from the central US to Alaska, in rough agreement with the results of the linear regression analysis. The anomalies linked to the SO high phase are not as coherent and areas of statistical significance are reduced. There is no evidence of a systematic impact of the SO over the western US. Symmetric relationships are present over the southeast and central regions as well as Alaska. Over Europe, there is no significant signal, in SAT or rainfall, associated with the SO low phase. In contrast, warm SAT anomalies are associated with the SO high phase over northern Europe to Siberia while cold anomalies occur over Baffin island and western Greenland, resulting in a temperature seasaw at high latitude. Close inspection of the high-latitude temperature signal reveals that it strongly projects onto the one associated with the positive phase of the NAO. As for precipitation, the SO high phase appears to be associated with a meridional dipole (with positive anomalies over northern Europe and negative ones over southern Europe and the Mediterranean), reminiscent of the pattern linked to the NAO positive phase cluster. However, areas with statistical significance are concentrated at the dipole meridional boundaries (north of the British Isles and Northern Scandi-

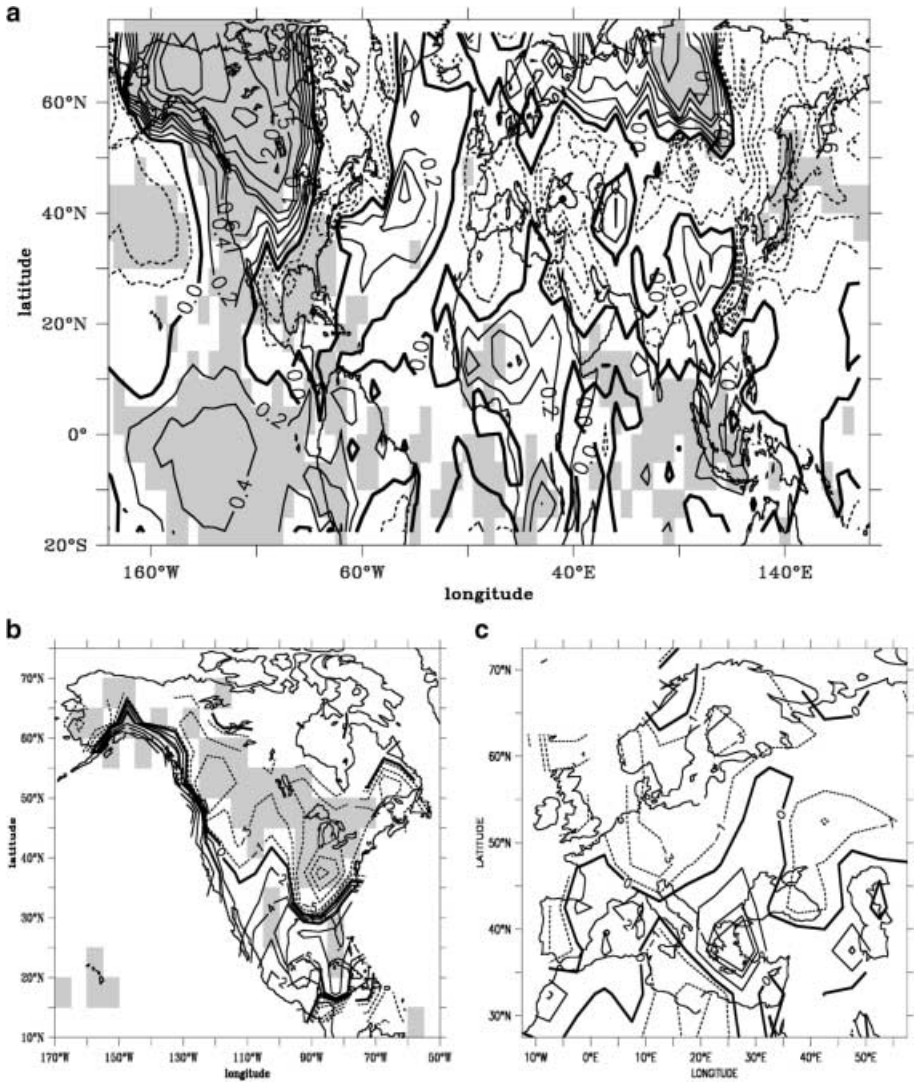

Fig. 10a–c. Patterns of winter (**a**) Northern Hemisphere land surface air and sea surface temperature and (**b, c**) land precipitation for the Pacific North American and North Atlantic-European sectors, respectively, associated with the cluster representing the negative phase of the SO (Fig. 9a). Shading indicates the regions where both the mean and variance of the climate variable composite are significant at the 95% level. Units are in K and mm

navia on one hand, southern Spain and Portugal and over the Adriatic region on the other hand) in contrast with Fig. 7c. These results reveal a significant regional response over Europe only for the SO high phase, questioning the climate system linearity with respects to opposite phases of the ENSO mode. They indicate enhanced anticyclonic activity over Europe during cold ENSO events (SO high phase) linked to higher temperature and precipitation over northern Europe. These surface climate anomalies are caused by the northward shift of the tail end of the North Atlantic storm track and its associated frontal systems. So the clustering analysis suggests that a statistically significant response of the NAE

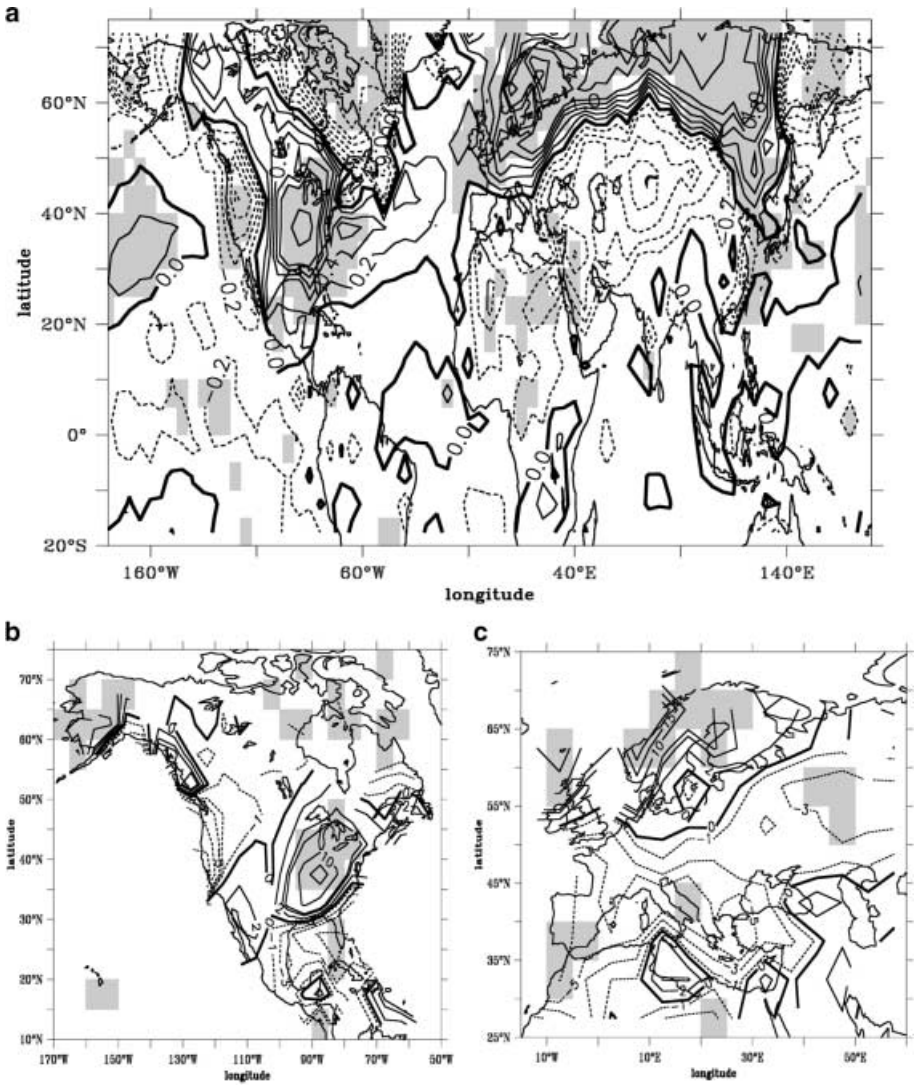

Fig. 11a–c. Patterns of winter (**a**) Northern Hemisphere land surface air and sea surface temperature and (**b, c**) land precipitation for the Pacific North American and North Atlantic-European sectors, respectively, associated with the cluster representing the positive phase of the SO (Fig. 9b). Shading indicates the regions where both the mean and variance of the climate variable composite are significant at the 95% level. Units are in K and mm

sector to the ENSO forcing exists only in the cold event case, adding complexity to the yet unresolved issue of a potential ENSO–Europe link (Rogers, 1984). A possible mechanism for this NAE sector response to La Niña events might involve first an initial perturbation in the west Atlantic basin due to the PNA arching pattern or a more direct impact on the Hadley circulation. This perturbation can influence the North Atlantic cyclogenesis and initiate a positive feedback through mean flow-transient eddies interactions. It then contributes to the maintenance and amplification of an initial high pressure anomaly in the subtropical North Atlantic (Fraedrich, 1994). The dependence of the anomalous eddy forcing to the

basic state might explain the non linearities of the response. This hypothesis can be explored with idealized models as in Peng and Whitaker (1999) for the midlatitude SST problem. Causes for this non linear response to the ENSO forcing might also be due to the different nature (regional or hemispheric) of the relevant modes of atmospheric circulation variability. The striking geographical similarity between the climate anomalies related to the SO high phase and those linked to the positive phase of the NAO strongly suggest that the clustering analysis have identified the regional signatures of a more zonally symmetric hemispheric mode of variability. Recently, Thompson and Wallace (1998, 1999) (hereafter TW98, TW99) have suggested that the NAO might be more appropriately viewed as an annular mode, the AO, characterized by a seasaw of atmospheric mass between the polar cap and the middle latitudes in both the Atlantic and Pacific basins. This is coherent with the spatial patterns of the two appropriate SLP clusters (the SO high phase and NAO positive phase ones) resulting from the analysis over the NPA and NAE sectors. Furthermore, the surface thermal signature of the positive polarity of the AO (Fig. 10 of TW99) is virtually identical to the ones of positive polarities of the SO and NAO. TW98 have shown that this zonally asymmetric temperature pattern is induced by the land-sea distribution and TW99 have suggested that horizontal temperature advection plays a major role in maintaining these SAT anomalies. While TW98 and TW99 have used essentially linear methods (EOF-based or linear correlation), application of clustering analysis has led to a slightly different viewpoint regarding the partition of northern hemisphere atmospheric variability modes. Application of the clustering analysis over the whole Northern Hemisphere led to almost similar results: one cluster exhibits north–south oriented dipoles in both the Pacific and the Atlantic with the northern pole having zonally elongated negative anomalies and the southern pole having much more localized positive anomalies (not shown). This cluster resembles the juxtaposition of the SO high phase and NAO positive phase clusters. A second one emerges with the opposite pattern in the Atlantic but without strong signature over the Pacific and is similar to the NAO negative phase cluster. Similar conclusions were reached using the NCEP reanalysis, suggesting the stability of the cluster repartition. So, according to our results, the contrasting polarities of the AO annular mode have different spatial features. The positive index one has an hemispheric pattern while the negative one has a more regional signature (localized over the NAE sector). Whether this is just a conceptual difference or reveals an intrinsic feature of Northern Hemisphere climate variability must await more in-depth analysis with other datasets, different clustering algorithms or other non linear methods.

4
Nature of the low-frequency variability modes and potential predictability of seasonal climate variables

While the coupled nature of the ENSO phenomenon is well established, the question is still opened regarding the NAO. The fundamental dynamics and mechanisms of the NAO seem to arise from purely atmospheric processes. The NAO appears to be a preferred mode of atmospheric variability whose position and spatial structure are related to the characteristics of the large-scale flow (Marshall and Molteni, 1993). Figure 12a, b compares the first mode of winter MSLP variability for the NAE region (through an EOF analysis) of the NCEP reanalysis with that of the ARPEGE model forced over 100 years by climatological SSTs. Both patterns are reminiscent of the NAO and the agreement, as far as amplitude and spatial structure, is quite remarkable between the two modes. The

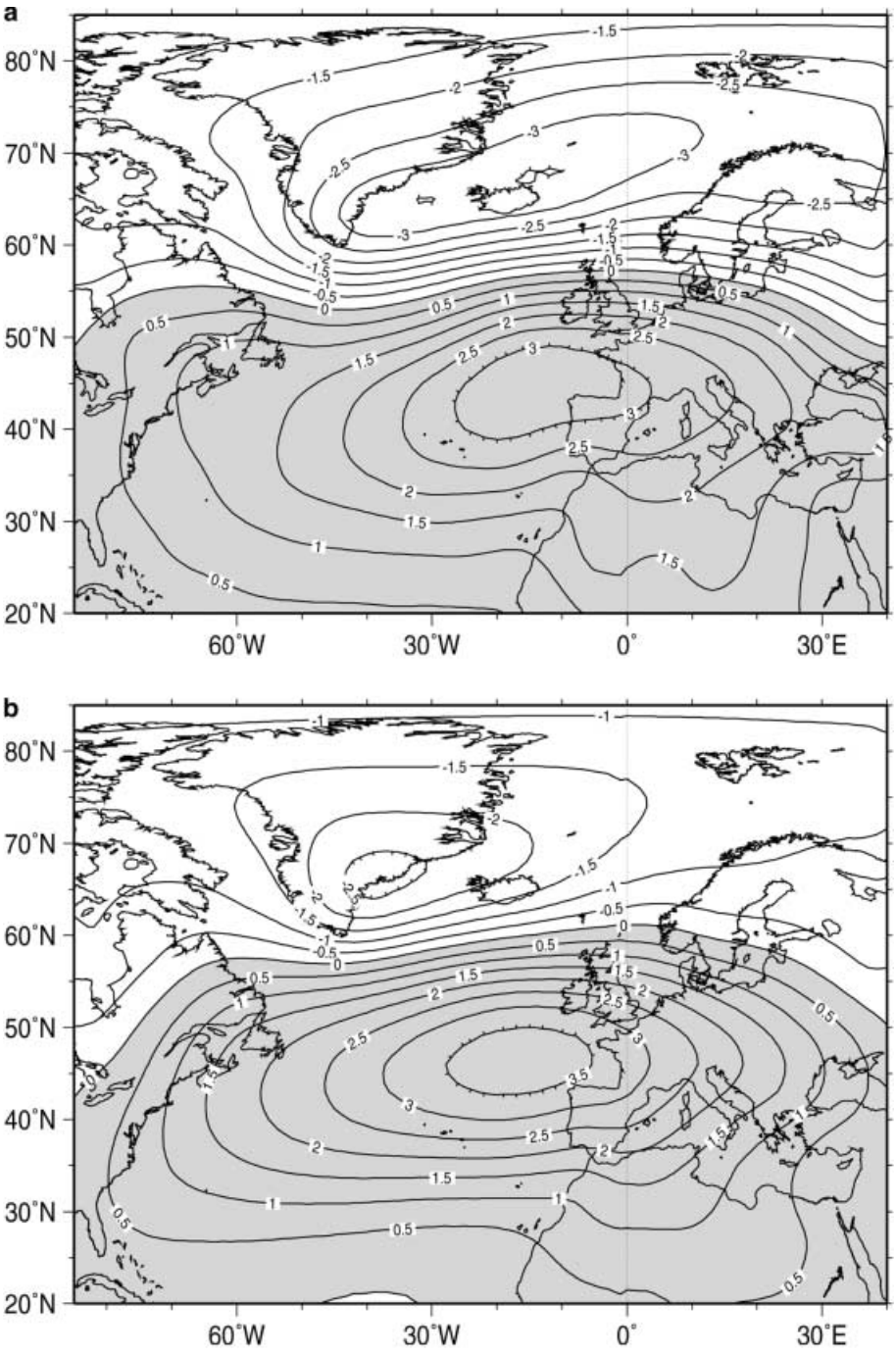

Fig. 12a–d. Spatial pattern of the first EOF of the temporal covariance matrix and spectrum of the associated principal component of the winter mean sea level pressure over the North Atlantic-European sector for (**a, c**) the NCEP reanalysis and (**b, d**) the ARPEGE model forced by climatological SSTs

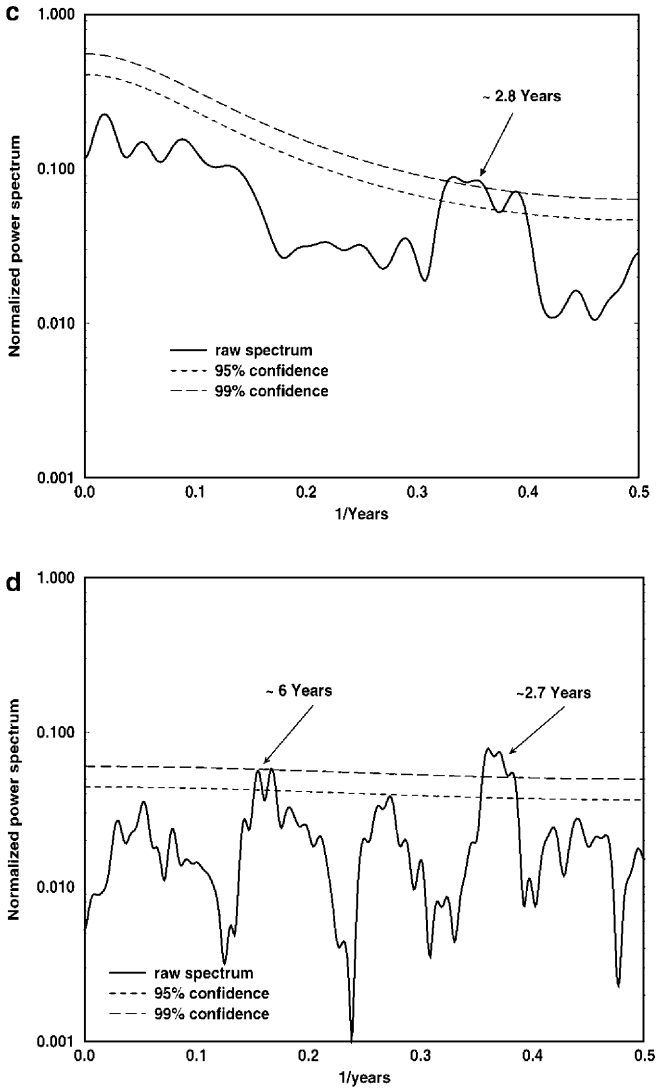

Fig. 12a–d. (Contd).

amount of explained variance by the first mode is also identical for the model and NCEP datasets (about 50%). While these results confirm that the primary NAO mechanisms are intrinsically atmospheric, they do not indicate whether atmospheric processes alone can lead to low-frequency variability over the Atlantic basin. Examination of the associated PCs spectra (Fig. 12c, d) shows that the model's PC has a flat spectrum (characteristic of a white noise process) with a quasi-biennal peak at 2.7 years. Conversely, the NCEP PC spectrum is much redder with also a broad-band peak centered around 2.8 years. These results suggest that intrinsic atmospheric processes cannot account for the energy concentration seen in the reanalysis data at near to interdecadal timescales. Furthermore, they indicate that the marked quasi-biennal fluctuations over the North Atlantic are primarily an atmospheric phenomenon. Various deterministic processes have been proposed to explain the increased power at low frequencies in

the NAOI spectrum: coupling with the ocean dynamics and thermodynamics, interaction with the stratosphere through vertically propagating planetary waves and global warming (Grötzner et al., 1998; Perlwitz and Graf, 1995; Shindell et al., 1999). On the other hand, the statistical properties of the NAOI timeseries are consistent with those of a long-range dependence process which could result from the aggregation of many stochastic weather synoptic events (Stephenson et al., 2000). Distinction between all these different possibilities is difficult to identify in the observed data alone and must be explored through modelling and theoretical work.

As an example, the following section presents an estimation of the influence of SST variability on the seasonal distribution of surface air temperature and rainfall from atmospheric-only simulations. In what follows, one is interested in the fraction of climate variability that is fully determined once the SST is known. It will be referred to as the climate signal by opposition to the noise, i.e. the internal and unpredictable component of the atmospheric variability. This SST-forced climate signal is often investigated using ensemble simulations of AGCMs forced with observed SSTs for multidecadal periods. The different members of the ensemble are started with different initial conditions. The main measure to characterize the SST influence is the spread or reproducibility between the different members of the ensemble. It can be determined using the analyse of variance method (ANOVA) which compares the variance between all the runs and the interannual variance of the ensemble mean. Here, the ANOVA method described by Rowell (1997) will be used to quantify the so-called atmospheric potential predictability which is defined as the ratio of the SST-forced variance to total variance of a given atmospheric field. All the assumptions, the algorithm and statistical testing are thoroughly detailed in Rowell (1997) to which the reader is referred to for an exhaustive description of the method. An ensemble of eight 50-year simulations were performed with the ARPEGE model previously described (Cassou and Terray, 2000). Each integration runs from 1 January 1947 to 31 March 1998, with the first year of each simulation being discarded because of possible spinup effects as the model atmosphere evolves from its initial state to one in quasi-equilibrium with the fixed SSTs. The observed surface ocean data used to force the GCM is the 2.3 version of the Global sea-Ice and Sea Surface Temperature (GISST) data set, described by Rayner et al. (1995).

Maps of potential predictability (PP) have been derived by applying the ANOVA technique at each model grid-point to the eight 50-year integrations and taking seasonal mean surface air temperature or precipitation as the seasonal characteristic whose variability is being assessed. Figure 13 shows ANOVA values for model 2 m air temperature in the four standard seasons. PP is high over the Tropics with values above 80% over the oceans and reaching over 60% over the tropical continents in all seasons. Values over North America are moderate but significant in winter and spring (generally 10–20% with maxima of 50%). In winter, significant values are found over Alaska and eastern Canada as well as in the southeastern US. In spring (season with maximum PP), high values are also found over the western, southern and eastern US while eastern Canada PP has decreased from the winter season. Values over Europe are generally 5–10% with slightly higher values in spring over the United Kingdom, Scandinavia and the Mediterranean. Over coastal Europe, temperature does have weak but significant PP values, in spring for northern Europe and summer for the southern part. This is probably due to the direct influence of the nearby specified SSTs. Over the extratropical oceans, PP is indeed much higher with values up to 80% in summer over the North Pacific and Atlantic.

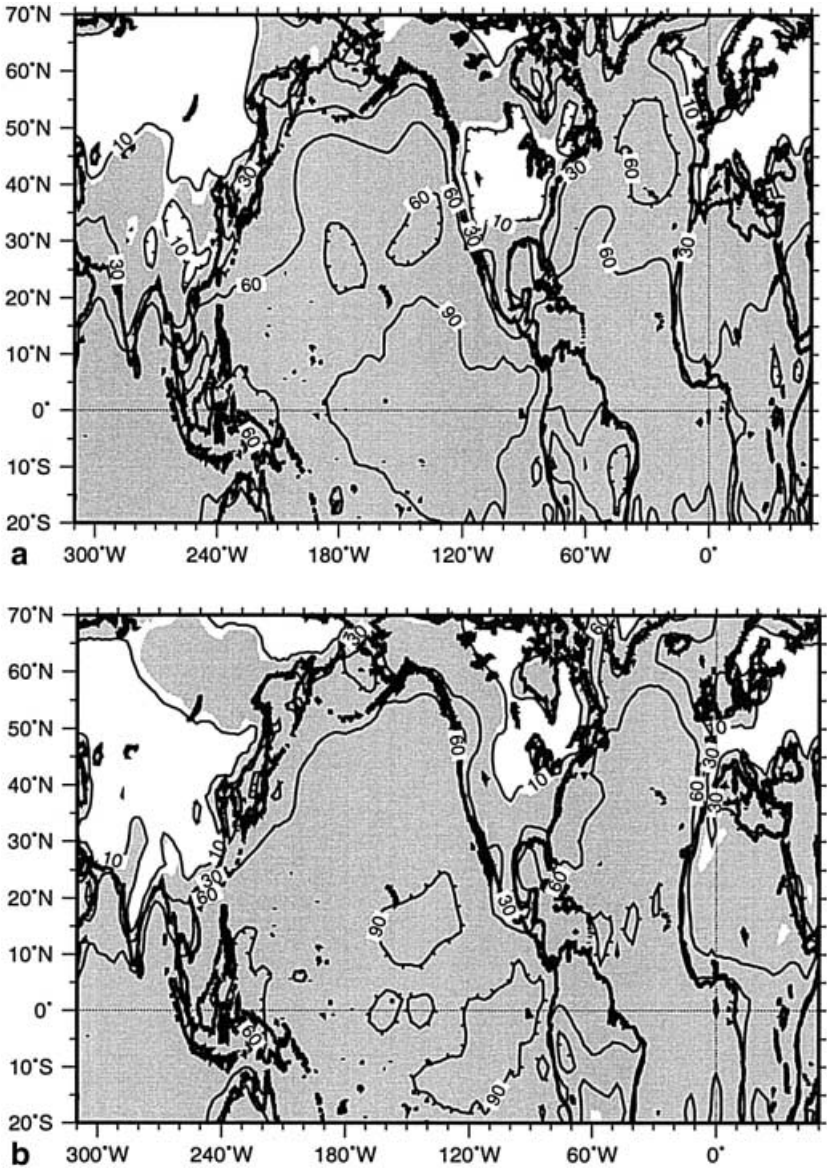

Fig. 13a–d. Percentage of total variance caused by SST and sea-ice forcing for seasonal 2 m temperature during 1948–1997. (**a**) DJF, (**b**) MAM, (**c**) JJA and (**d**) SON. Shading indicates areas where values are significantly different from zero at the 95% level

Similar maps for precipitation (not shown) yield lower variance values over North American and European land areas (0–10%) with maxima of 25% over the southeastern US in winter and spring and 15% over the Mediterranean in fall and winter. Areas of significant ocean SST influence are smaller than those for surface air temperature. The weak potential predictability over Europe is a recurrent feature from ANOVA analysis of AGCMs ensemble integrations (Davies et al., 1997). This indicates that the modulation of European climate variability by the oceanic forcing is certainly smaller than the midlatitude internal variability.

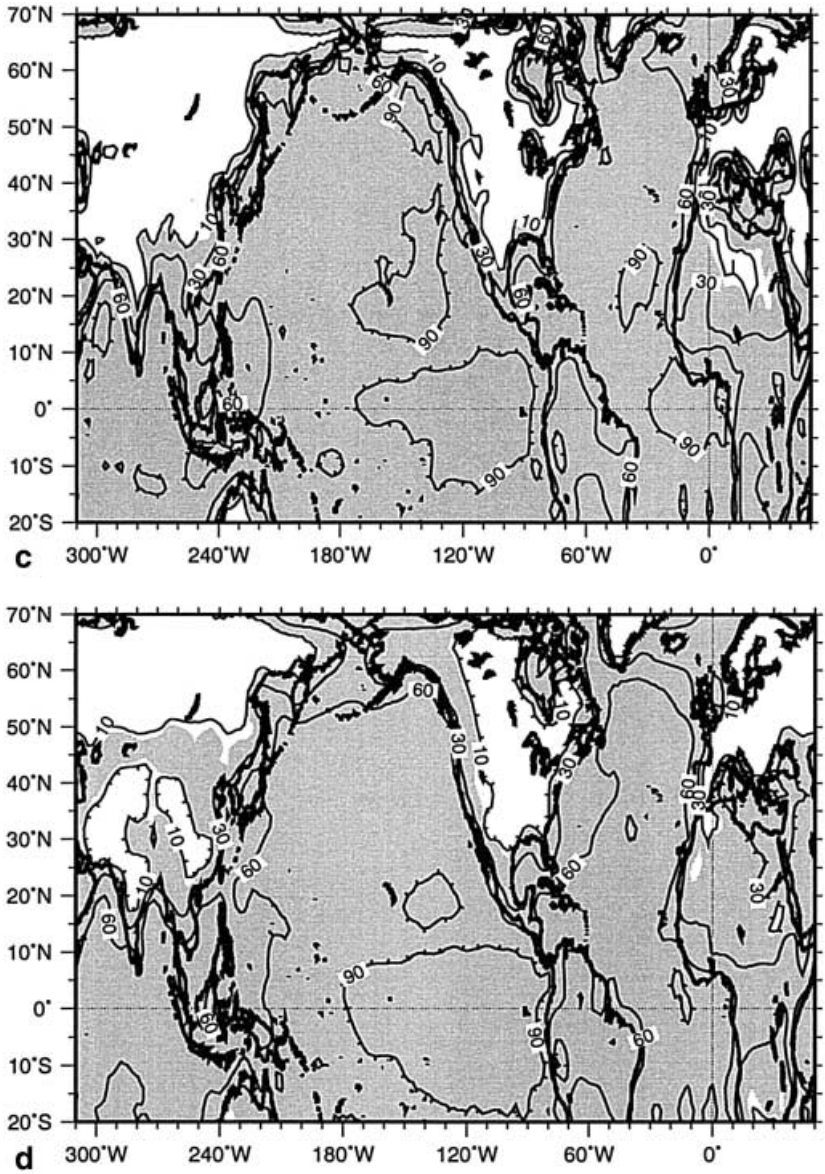

Fig. 13a–d. (Contd).

However, definite statements about the relevance of seasonal to interannual prediction over the European sector must await until a better understanding of tropics-extratropics as well as midlatitude coupled air–sea interactions and related improvements in physical parameterizations have occurred.

5
Interaction between global warming and the low-frequency variability modes

This section provides a short review of selected works published recently about the relationships between the recent climatic trends and the low-frequency

►

Fig. 14a–c. Multi-decadal observed winter trend over the Northern Hemisphere sector for (**a**) mean sea level pressure (period 1962–1993), (**b**) land surface air and sea surface temperature (period 1962–1993) and (**c**) land precipitation (period 1962–1993). Significant areas at the 95% level are coloured (significance assessed with the Mann–Kendall test). Units are 1 hPa/32-years for MSLP, 1 K/32-years for temperature and 1 mm/32-years for precipitation

modes of atmospheric variability. Global mean surface temperatures have risen between 0.3° and 0.6 °C over the past century, including a warming of 0.2° to 0.3 °C since the 1950s when data are the most reliable (IPCC, 1995). Recent studies have suggested that this increase in global mean temperature may be associated with anthropogenic changes in atmospheric composition. Since global mean temperatures are dominated by temperature variability over the northern continents, a significant fraction of the recent observed warming can be explained as a response to observed changes in atmospheric circulation. As shown by Fig. 1, important changes in the wintertime atmospheric circulation have occurred since the late 1960s over the ocean basins of the Northern Hemisphere. The SOI for the winter months illustrates a change towards more negative values from the 1970s onward. The winter NAOI exhibits a similar trend, going from the negative values of the 1960s to the record-level positive values of the 1990s. Inspection of the linear trends in MSLP, surface temperature and precipitation (Fig. 14) over the 1962–1993 winter period shows strong similarity to the regional patterns associated with the low frequency variability modes, in particular with the NAO. The MSLP trend is characterized by falling heights over most of the Arctic basin and eastern Eurasia. The pattern over the North Atlantic strongly projects on the NAO positive phase pattern. There is also MSLP increase over the Mediterranean region and the subtropical Atlantic. The trend in SAT is dominated by strong warming over the high latitude continents with maxima over Siberia, northern Europe and western Canada, and weaker cooling over Greenland and Labrador. The SST trend depicts the SST tripole associated with the NAO positive phase. The negative center in the Greenland and Labrador seas is well marked while the two others are weaker and localized near the coast. There is weak cooling over the North Pacific and warming off the west coast of the US. The trends in precipitation have features of smaller scale and not as coherent as those for SLP and surface temperature. The main regional patterns are the precipitation increases over Northern Europe, Central Eurasia, Alaska and northern Mexico and the decreases over southern Europe, north-eastern Asia and central North America. The reader is referred to Hurrel (1995, 1996) and Thompson et al. (1999) and references therein for more detailed description of the recent trends and their links with the NAO and the AO. The striking similarity between the regional features of the low frequency climate trends and the signature of the annular mode as depicted by the clustering analysis suggests the following possibility: anthropogenic climate change, perhaps through interaction with the stratosphere) might bias the distribution of climate states towards the annular mode (i.e. positive index of the AO or NAO) (Corti et al., 1999). Much more work is needed to understand how the natural modes of low-frequency variability may be influenced by climate change. There is no doubt that atmospheric modelling linked to climate change studies must focus on improved physical description of the stratosphere and inclusion of stratospheric chemical processes involving chlorine and ozone.

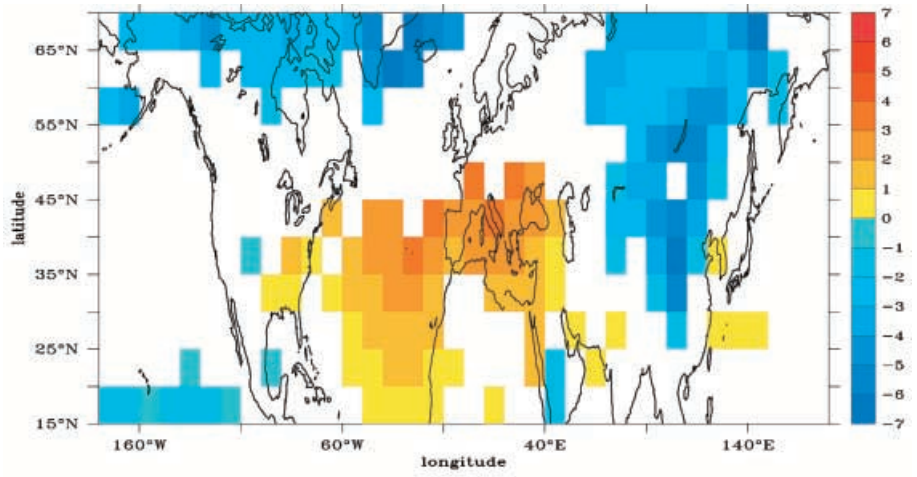
65°N
55°N
45°N
35°N
25°N
15°N
latitude
160°W
60°W
40°E
140°E
longitude
7
6
5
4
3
2
1
0
−1
−2
−3
−4
−5
−6
−7

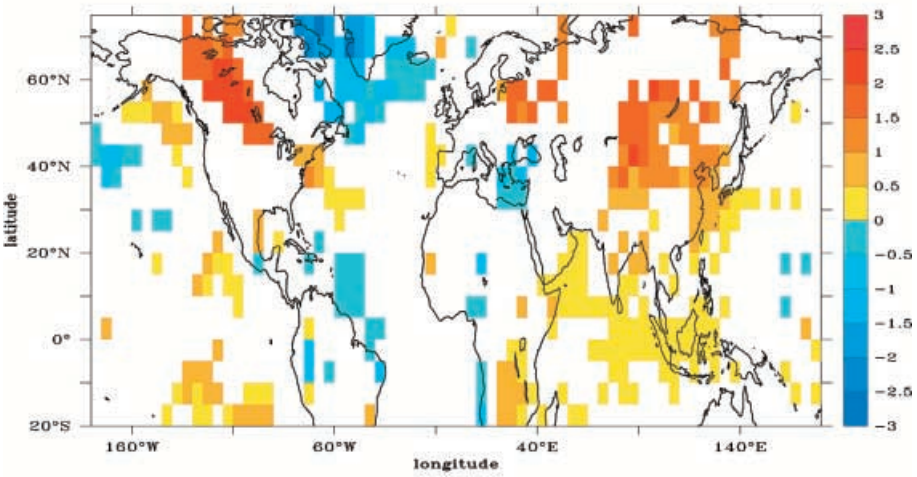
60°N
40°N
20°N
0°
20°S
latitude
160°W
60°W
40°E
140°E
longitude
3
2.5
2
1.5
1
0.5
0
−0.5
−1
−1.5
−2
−2.5
−3

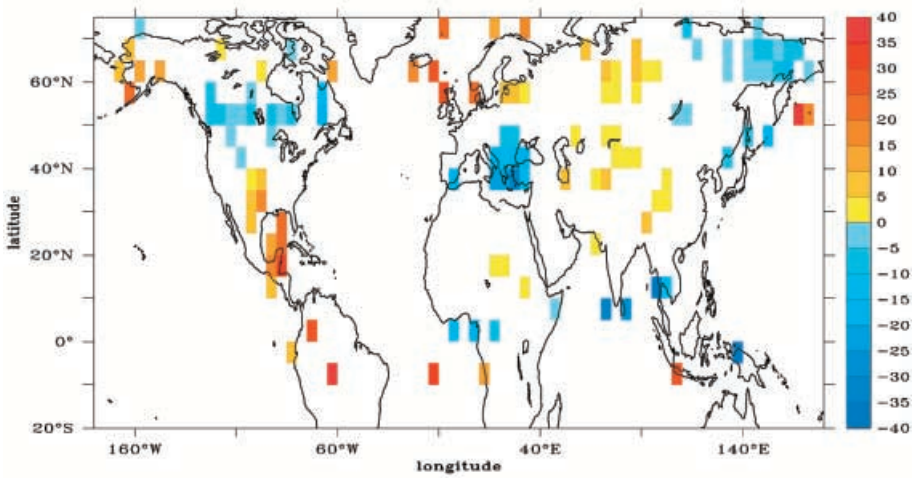
60°N
40°N
20°N
0°
20°S
latitude
160°W
60°W
40°E
140°E
longitude
40
35
30
25
20
15
10
5
0
−5
−10
−15
−20
−25
−30
−35
−40

6
Conclusions

In the first part of this study, two primary approaches were used to identify observed relationships between low-frequency climate variability modes and geographical distributions of winter surface temperature and land precipitation anomalies over the Northern Hemisphere. Two of these modes have been selected for the present study: the SO and the NAO. As this paper deals primarily with the midlatitudes, the SO and its related teleconnection patterns as well as the NAO were investigated.

In the first approach, the time history of the modes of low-frequency climate variability are defined using MSLP indexes, the SOI and NAOI, which depict changes in the large-scale atmospheric circulation. The signatures of these modes on land rainfall and surface temperature are then estimated using linear regression between the SOI and NAOI and the various global fields over the last century. The second approach, which overcomes the limitations of linear regression, is based on clustering analysis. The algorithm has been applied to the winter MSLP field over both the NPA and NAE sectors.

The main results support the following conclusions:

- Spectral analysis shows that while the SOI has a clear peak around 4 years, the NAOI spectrum is quasi white with slight broadband features near biennal and decadal time scales. Furthermore, the two time series exhibit recent and marked trends which seem to exceed both the high frequency noise and the interdecadal variability observed during the last century.
- The clusters representing contrasting polarities of the NAO are associated with surface temperature and land rainfall patterns which strongly resemble their linear counterparts. The anomaly patterns show the well-known temperature seasaw between the northwest Atlantic and Europe as well as the meridional precipitation dipole between Scandinavia and southern Europe.
- The NAE sector response to the SO is strongly non linear. There is no significant response associated with the SO low-phase while the SO high-phase one strongly projects onto the patterns (for both SAT and land rainfall) related to the NAO positive phase. This supports the recent studies by TW98 and TW99 about the existence and relevance of the annular modes. However, the clustering analysis (which accounts for non linearities) suggests that this viewpoint is well adapted only in the case of the SO high-phase – NAO positive phase couple. In contrast, the cluster associated with the SO low-phase has a more localized pattern and no significant teleconnection to the NAE sector.

The second part of this study investigates the nature of the NAO and the potential predictability of climatic variables using atmospheric model experiments. The following conclusions can be drawn from these studies:

- EOF-analysis of a long forced atmospheric integration with climatological forcing supports the view of the intrinsic nature of the NAO which seems to be a preferred mode of atmospheric variability over the NAE sector. However, it also suggests that the atmosphere on its own is unable to generate the low frequency energy concentration seen in the observed data over the last century. To explain the shape of the energy spectrum, one has to invoke the influence of another player, be it the ocean and long-term changes associated with the thermohaline circulation or the anthropogenic influence through troposphere-stratosphere interactions.

- Values of externally forced variance, as deduced from an ANOVA analysis of a multidecadal ensemble of AGCM integrations, are usually weak over the mid-to-high latitudes continental regions of the Northern Hemisphere, confirming the predominance of quasi-stochastic internal variability. The model shows the most predictable seasons for land surface temperature and precipitation over the NAE to be winter and spring. For temperature, there are weak but significant PP maxima in winter over Canada and the southern US while the signal is marginal over Europe. In spring, there are significant PP maxima over the western, southern and eastern US as well as over the UK and the southern tip of Europe.

Finally, the low-frequency climate trends estimated over the last 30 years are consistent with the regional features associated with the NAO positive phase and SO high phase clusters: milder winters in Eurasia and western Canada, more severe winters over Greenland and eastern Canada as well as reduced precipitation in southern Europe and the Middle East, heavier rainfall over northern Europe, Central Eurasia, Alaska and the Gulf of Mexico region. The striking similarity of these patterns might indicate that the recent climate trends, whether their origin is anthropogenic or not, originate from a change in the repartition of the different atmospheric circulation regimes. The primary cause of the trend in the annular mode has yet to be determined unambiguously among the various postulated mechanisms: stratospheric ozone depletion, greenhouse gases and aerosols concentration increase, intrinsic ocean variability or volcanic eruptions.

References

Appenzeller C, Schwander J, Sommer S, Stocker TF (1998) The North Atlantic Oscillation and its imprint on precipitation and ice accumulation in Greenland. Geophys. Res. Lett., 25: 1939–1942

Barnston AG, Livezey RE (1987) Classification, seasonality and persistence of low-frequency atmospheric circulation patterns. Mon. Wea. Rev., 115: 1083–1126

Bjerknes J (1964) Atlantic air-sea interaction. Adv. Geophys., 10: 1–82

Bjerknes J (1969) Atmospheric teleconnections from the equatorial Pacific. Mon. Wea. Rev., 97: 163–172

Bougeault P (1985) A simple parameterization of the large-scale effects of deep cumulus convection. Mon. Wea. Rev., 113: 2108–2121

Bretherton CS, Smith C, Wallace JM (1992) An intercomparison of methods for finding coupled patterns in climate data. J. Climate, 5: 541–560

Cassou C, Terray L (2000) Influence of tropical and extratropical SST anomalies on interannual atmospheric variability over the North Atlantic-European sector. J. Climate, in press

Cheng X, Wallace JM (1993) Cluster analysis of the Northern hemisphere wintertime 500 hPa height field: spatial patterns. J. Atmos. Sci., 50: 2674–2696

Cook ER, D'Arrigo RD, Briffa KR (1998) A reconstruction of the North Atlantic Oscillation using tree-ring chronologies from North America and Europe. The Holocene, 8(1): 9–17

Corti S, Molteni F, Palmer TN (1999) Signatures of recent climate change in frequencies of natural atmospheric circulation regimes. Nature, 398: 799–802

Cullen HM, deMenocal PB (1999) North Atlantic influence on Turkish climate and water supply. Int. J. Climatol., in press

Davies JR, Rowell DP, Folland CK (1997) North Atlantic and European seasonal predictability using an ensemble of multidecadal AGCM simulations. Int. J. Climatol., 17: 1263–1284

Déqué M, Dreveton C, Braun A, Cariolle D (1994) The climate version of Arpege/IFS: a contribution to the French community climate modelling. Clim. Dyn., 10: 249–266

Deser C, Blackmon ML (1993) Surface climate variations over the North Atlantic ocean during winter. J. Climate, 6: 1743–1753

Dettinger MD, Ghil M, Strong CM, Weibel W, Yiou P (1995) Software expedites singular-spectrum analysis of noisy time series. Eos Trans. American Geophysical Union, 76(2): 12, 14, 21

Dunbar RB, Wellington GM, Colgan MW, Glynn PW (1994) Eastern Pacific sea surface temperature since 1600 AD: The δ^{18}O record of climate variability in Galapagos corals. Paleoceanography, 9: 291–316
Fraedrich K (1994) An ENSO impact on Europe? A review. Tellus, 46A: 541–552
Grötzner AM, Latif M, Barnett TP (1998) A decadal climate cycle in the North Atlantic ocean as simulated by the ECHO coupled GCM. J. Climate, 11: 831–847
Halpert MS, Ropelewski CF (1992) Surface temperature patterns associated with the Southern Oscillation. J. Climate, 5: 577–593
Horel JD, Wallace JM (1981) Planetary scale atmospheric phenomena associated with the Southern Oscillation. Mon. Wea. Rev., 109: 813–829
Hulme M (1992) A 1951–80 global land precipitation climatology for the evaluation of General Circulation Models. Clim. Dyn., 7: 57–72

Hurrel JW (1995) Decadal trends in the North Atlantic Oscillation and relationships to regional temperature and precipitation. Science, 269: 676–679
Hurrel JW (1996) Influence of variations in extratropical wintertime teleconnections on Northern Hemisphere temperature. Geophys. Res. Lett., 23: 665–668
Hurrel JW, Van Loon H (1997) Decadal variations in climate associated with the North Atlantic Oscillation. Climatic Change, 36: 301–326
Jones PD (1987) The early twentieth century Arctic High – fact or fiction? Clim. Dyn., 1: 63–75
Jones PD (1994) Hemispheric surface air temperature variations: a reanalysis and an update to 1993. J. Climate, 7: 1794–1802
Jones PD, Raper SC, Bradley RS, Diaz HF, Kelly PM, Wigley TML (1986) Northern Hemisphere surface temperature variations, 1851–1984. J. Clim. Appl. Met., 25: 161–179
Jones PD, Jónsson T, Wheeler D (1997) Extension to the North Atlantic Oscillation using early instrumental pressure observations from Gibraltar and South-West Iceland. Int. J. Climatol., 17: 1433–1450
Kalnay E, et al. (1996) The NCEP/NCAR 40-year reanalysis project. Bull. Amer. Meteor. Soc., 77: 437–471
Kiladis GN, Diaz HF (1989) Global climatic anomalies associated with extremes in the Southern Oscillation. J. Climate, 2: 1069–1090
Lamb PJ, Peppler RA (1991) West Africa. Teleconnections linking worldwide climate anomalies. In: Glantz M, Katz RW, Nicholls N (Eds.) Cambridge University Press, pp. 121–189
Louis JF, Tiedke M, Geleyn JF (1982) A short history of the operational PBL parameterization at ECMWF. Proc. ECMWF workshop on planetary boundary layer parameterization, Reading, ECMWF, pp. 59–80
Mann ME, Lees J (1996) Robust estimation of background noise and signal detection in climatic time series. Climate Change, 33: 409–445
Marshall JC, Molteni F (1993) Towards a dynamical understanding of weather regimes. J. Atmos. Sci., 50: 1792–1818
Martineu C, Caneill JY, Sadourny R (1999) Potential predictability of european winters from the analysis of seasonal simulations with an AGCM. J. Climate, 12: 3033–3061
Morcrette JJ (1990) Impact of changes to the radiation transfer parametrizations plus cloud optical properties in the ECMWF model. Mon. Wea. Rev., 118: 847–873
Noilhan J, Planton S (1989) A simple parameterization of land surface processes for meteorological models. Mon. Wea. Rev., 117: 536–549
Parker DE, Folland CK, Jackson M (1995) Marine surface temperature: observed variations and data requirements. Climatic Change, 31: 559–600
Peng S, Whitaker JS (1999) Mechanisms determining the atmospheric response to midlatitude SST anomalies. J. Climate, 12: 1393–1408
Perlwitz J, Graf HF (1995) The statistical connection between tropospheric and stratospheric circulation of the northern hemisphere in winter. J. Climate, 8: 2281–2295
Quiroz RS (1983) The climate of the El Niño winter of 1982–83 – A season of extraordinary climatic anomalies. Mon. Wea. Rev., 111: 1685–1706
Rayner NA, Folland CK, Horton B, Parker DE (1995) A new Global sea Ice and Sea Surface Temperature (GISST) data set for 1903–1994'. Presented by C.K. Folland to the Wadati Conference on Global Change and the Polar Climate, Tsukuba, Japan, 7–10 November 1995. Available as Hadley Centre Internal note No 69

Rogers JC (1984) The association between the North Atlantic Oscillation and the Southern Oscillation in the northern hemisphere. Mon. Wea. Rev., 112: 1999–2015
Rogers JC (1990) Patterns of low-frequency monthly sea level pressure variability (1899–1986) and associated wave cyclone frequencies. J. Climate, 3: 1364–1379
Ropelewski CF, Jones PD (1987) An extension of the Tahiti-Darwin Southern Oscillation Index. Mon. Wea. Rev., 115: 2161–2165
Rowell DP (1997) Assessing potential seasonal predictability with an ensemble of multi-decadal GCM simulations. J. Climate, 11: 109–120
Shindell DT, Miller RL, Schmidt GA, Pandolfo L (1999) Simulation of recent northern winter climate trends by greenhouse-gas forcing. Nature, 399: 452–455
Stephenson DB, Pavan V, Bojariu R (2000) Is the North Atlantic Oscillation a random walk? Int. J. Climatol., 20: 1–18
Sutton RT, Allen MR (1997) Decadal variability of North Atlantic sea surface temperature and climate. Nature, 388: 563–567
Thompson DJ (1982) Spectrum estimation and harmonic analysis. IEEE Proc., 70: 1055–1096
Thompson DWJ, Wallace JM (1998) The arctic oscillation signature in the wintertime geopotential height and temperature fields. Geophys. Res. Lett., 25: 1297–1300
Thompson DWJ, Wallace JM (1999) Annular modes in the extratropical circulation Part I: month-to-month variability. J. Climate, 13: 1000–1016
Thompson DWJ, Wallace JM, Hegerl GC (1999) Annular modes in the extratropical circulation Part II: trends. J. Climate, 13: 1018–1036
Trenberth KE, Shea DS (1987) On the evolution the Southern Oscillation. Mon. Wea. Rev., 115: 3078–3096
Trenberth KE, Hurrel JW (1994) Decadal atmosphere-ocean variations in the Pacific. Climate Dyn., 9: 303–319
Van Loon H, Madden R (1981) The Southern Oscillation. Part 1: global associations with pressure and temperature in northern winter. Mon. Wea. Rev., 109: 1150–1162
Van Loon H, Rogers JC (1978) The Seasaw in winter temperature between Greenland and northern Europe. Part 1: general description. Mon. Wea. Rev., 106: 296–310
Vautard R, Yiou P, Ghil M (1989) Singular-spectrum analysis: a toolkit for short noisy chaotic signals. Physica D, 58: 95–126
Walker GT (1924) Correlation in seasonal variations of weather. IX, A further study of world weather. Mem. Indian Meteorol. Dep., 24(9): 275–332
Walker GT, Bliss EW (1932) World Weather V. Mem. Roy. Meteor. Soc., 4: 53–84
Wallace JM, Gutzler DS (1981) Teleconnections in the geopotential height field during the Northern Hemisphere winter. Mon. Wea. Rev., 109: 784–812
Wunsch C (1999) The interpretation of short climate records, with comments on the North Atlantic and Southern oscillations. Bull. Amer. Meteor. Soc., 80: 245–255